To our knowledge, this is the first report to show that vimentin can play a role in TGF-β activation by the LAP fragment.

2. Materials and methods

2.1. Materials

Peptide-25, Peptide-25N, N-terminally biotin-labeled peptide and Peptide-21 were synthesized as previously described [9]. Bovine aortic endothelial cells (BAECs) were cultured in Dulbecco's modified eagle medium containing 10% fetal bovine serum (FBS) as previously described.

2.2. Cross-linking of Peptide-25N to the target molecule using BAECs

The confluent monolayers were crosslinked with 100 μM Peptide-25N using 2 mM Sulfo-EGS (Pierce Biotechnology, Rockford, IL) and harvested in detachment buffer (DB; 0.25 M sucrose, 0.3 mM PMSF, 10 mM Tris, 1 mM EDTA, pH 7.4, 10 μg/mL of leupeptin, antipain, and pepstatin, 50 μg/mL aprotinin, 100 μg/mL soybean trypsin inhibitor, 10 μg/mL bestatin and benzamidin hydrochloride, and 300 μM PMSF). In some experiments, crosslinking of Peptide-25N to the suspended cells was performed as described above and the precipitated cells were suspended in DB. Samples were stocked at −20 °C. The cells stocked were thawed, precipitated, and solubilized in reducing sample buffer for SDS–PAGE. To purify the target molecule, the membrane fraction was obtained in supernatant by solubilization in the buffer containing 8.5 M urea and 2% Nonidet P-40 and centrifugation.

2.3. Purification of a target molecule by avidin–biotin affinity chromatography and SDS–PAGE

The membrane fraction was applied onto the avidin–biotin affinity chromatography column (Ultralink Immobilized Monomeric Avidin Gel, Pierce Biotechnology) equilibrated with starting buffer (SB: 1.25 M urea, 2% NP-40, 125 mM NaCl, 10 mM Tris, 1 mM EDTA, pH 7.4). After washing the column with SB, strongly bound molecules including the target molecule of Peptide-25N were eluted in the buffer (2 M urea, 2% NP-40, 125 mM NaCl, 100 mM glycine, pH 2.8). The target molecules fractionated by the avidin–biotin affinity chromatography were precipitated by incubation in cold acetone at −20 °C over night, centrifuged, dried in vacuo, and applied to SDS–PAGE. The bands corresponding to the target complex containing Peptide-25N and to the co-eluted protein were cut out and extracted in reducing sample buffer at 37 °C over night. The purity of the target molecule preparation was confirmed by SDS–PAGE with Ag-staining using 2D-Silver Stain II "DAIICHI" (Daiichi Pure Chemicals, Tokyo, Japan).

2.4. Detection of the complex containing Peptide-25N by avidin staining

The proteins separated on SDS–PAGE were blotted onto a polyvinylidene fluoride (PVDF) membrane (Millipore, Billerica, MA) and the complex containing Peptide-25N was detected using avidin-biotinylated horseradish peroxidase (HRP) complex solution (Elite Vectastain ABC kit; Vector Laboratories, Burlingame, CA) and visualized using ECL substrate solution and ECL film (Amersham Biosciences, Piscataway, NJ).

2.5. Amino acid sequencing of the co-eluted protein

The piece cut from the gel was applied to endoproteinase Asp-N (Roche Diagnostics GmbH, Mannheim, Germany) digestion and the produced peptide fragments were separated by RP-HPLC using a MIC-15-03-MRP column (LC PACKING, San Francisco, CA) on SMART system (Amersham). Fragments were applied to Edman degradation by a LC system (492cLC, Applied Biosystems Japan, Tokyo, Japan) and a protein sequencer (PPSQ-10, Shimadzu, Kyoto, Japan). The co-eluted protein was identified by the N-terminal sequence determination of the fragments followed by the comparison with protein database SWISS-PROT.

2.6. Western blot analysis with anti-vimentin monoclonal antibodies

The complex containing Peptide-25N, and the co-eluted protein extracted above were applied to SDS–PAGE followed by silver staining or Western blot analysis with anti-vimentin monoclonal antibody (mAb), clone V9 (ICN Pharmaceuticals, Aurora, OH), HRP-linked whole anti-mouse IgG., ECL substrate solution, and ECL film (Amersham).

2.7. Binding assay of Peptide-25N to immobilized vimentin protein

The wells of 96-well black plates coated with 2 μg/mL of bovine vimentin (PROGEN, Heidelberg, Germany) were blocked with PBS containing 1% bovine serum albumin (PBS-BSA) for 2 h. Five microgram per milliliters of anti-vimentin mAb VIM3B (IgG2a) (PROGEN) or anti-α-actin mouse mAb clone ASM-1 (IgG2a) (PROGEN), or vehicle and then Peptide-25N solution was added. The wells were incubated with HRP-conjugated avidin (Amersham) in BSA-PBS for 1 h. After each step, wells were washed. The wells were incubated with ELISA Pico (Pierce) for 5 min. The chemiluminescence was detected using a plate reader (EnVision 2102 Multilabel reader, Perkin Elmer, Waltham, MA). In some experiments, the soluble vimentin was added in the presence of 1 μM Peptide-25N.

2.8. FACS analysis

To detect surface proteins, BAECs were harvested non-proteolytically by cell dissociation buffer (GIBCO BRL, Carlsbad, CA) and not permeabilized. The first Ab was 5 μg/mL of anti-bovine vimentin mAb clone VIM3B4 (IgG2a) or of mouse IgG2a and the second Ab was 8 μg/mL of fluorescein isothiocyanate (FITC)-conjugated anti-mouse IgG2a Ab (Santa Cruz Biotechnology, Santa Cruz, CA). Intact living cells which excluded propidium iodide were analyzed by FACS Vantage (Becton Dickinson, Bedford, MA). The difference in vimentin expression was evaluated by Kolmogrov–Smirnov test.

2.9. Binding assay of Peptide-25N to BAECs

Binding assays using BAECs were performed at 37 °C as described previously [9]. BAECs plated in a 96-well black plate were preincubated with 5 μg/mL of anti-bovine vimentin mouse mAb (clone VIM3B4) or with vehicle for 30 min. Cells were incubated for 60 min with 100 μg/mL of biotin-labeled or unlabeled peptide and then in HRP-conjugated streptavidin (Amersham) for further 30 min. the amount of bound peptide was detected by the addition of ECL Western blotting detection reagent (Amersham) and measured by Luminescencer JNR (Atto Co., Tokyo, Japan).

2.10. Wound migration assay

Wound migration assays were performed as described previously [9]. Cells were incubated with 100 μg/mL of peptide in preincubation (6 h) and in incubation (24 h) step after wounding. In some experiments, 5 μg/mL of anti-vimentin mouse mAb clone V9 (IgG1) (NeoMarkers, Fremont, CA) or of mouse IgG1 were added in both steps.

2.11. Statistical analysis

The statistical significance of differences in the data was evaluated by use of analysis of variance (ANOVA) and P values were calculated by Tukey's method. For comparison of two groups, the t-test was used. A value of $P < 0.05$ was accepted as statistically significant.

3. Results

To identify the membrane protein of binding partner for Peptide-25, the cross-linking experiment combined with avidin staining was performed (Fig. 1) and revealed a specific band bound to Peptide-25N in BAECs (the arrow in lane 1). This band was not detected in the absence of Peptide-25 in spite of the presence of Sulfo-EGS, a cross-linker (lane 2). Therefore, we decided to purify and identify this band as the target molecule bound to Peptide-25.

The membrane fraction was applied to avidin–biotin affinity chromatography and then SDS–PAGE (Fig. 1B). This target molecule (band A) and a co-eluted protein (band B) were further purified by SDS–PAGE. Firstly, the co-eluted protein with the consistent molecular size of 55 kDa [10] was identified as vimentin as a result of amino acid sequencing. To confirm it, the bands A and B were applied to Western blot analysis (Fig. 2). The band A (lanes 9 and 10) and the band B (lanes 6–8) reacted with an anti-vimentin mAb (Fig. 2). This result was reproduced, when another anti-vimentin mAb, clone VIM3B4, was used (data not shown). Therefore, we concluded that the target molecule to which Peptide-25N bound was vimentin (band B) and band A was the complex of vimentin and Peptide-25N (about 2.7 kDa).

We found that binding of Peptide-25 to EC surface was the key step for the augmented binding and activation of latent TGF-β [9]. To clarify whether vimentin is involved in this phenomenon, firstly we performed the binding assay. Peptide-25N bound to the immobilized vimentin protein in a dose dependent manner and anti-vimentin mAb (IgG2a) inhibited it, whereas anti-α-actin mAb, an irrelevant IgG2a, did not (Fig. 3A). Soluble vimentin suppressed the binding of Peptide-25N in a dose-dependent manner (Fig. 3B). These results indicate that vimentin could be a binding partner of Peptide-25. Next, we conducted FACS analysis using

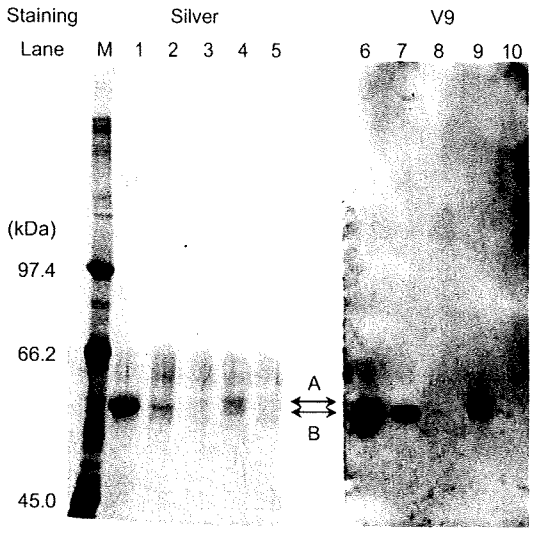

Fig. 2. Western blot analysis of the target fraction with anti-vimentin monoclonal antibody. Proteins from band A (lanes 4, 5, 9, and 10) and B (lanes 1–3 and 6–8) (Fig. 1B) were applied to SDS–PAGE followed by silver staining or Western blot analysis using anti-vimentin mAb, clone V9. The amount corresponding to culture area (cm^2): 119 for lanes 1, 4, 6, and 9; 11.9 for lanes 2, 5, 7, 10; 1.19 for lanes 3 and 8. The complex of Peptide-25N and its crosslinked protein, and the co-eluted protein were indicated by arrows A and B, respectively.

alive and membrane-intact BAECs and found that vimentin can exist on cell surface (Fig. 4A). Moreover, anti-vimentin mAb significantly suppressed the binding of peptide-25 to cells (Fig. 4B). These results indicate that Peptide-25 can directly and specifically interact with vimentin on cell surface.

Finally, we performed wound migration assay which is widely used to quantify activation of latent TGF-β [6,7,9,11,12]. Mature TGF-β, an active form, shows inhibitory activity to EC migration. Fig. 5 shows that Peptide-25 decreased the migration of ECs as we previously reported [9]. This inhibitory activity of Peptide-25 was attenuated by anti-vimentin mAb. In contrast to Peptide-25, Peptide-21 showed no significant activity (Fig. 5). Peptide-21 (from

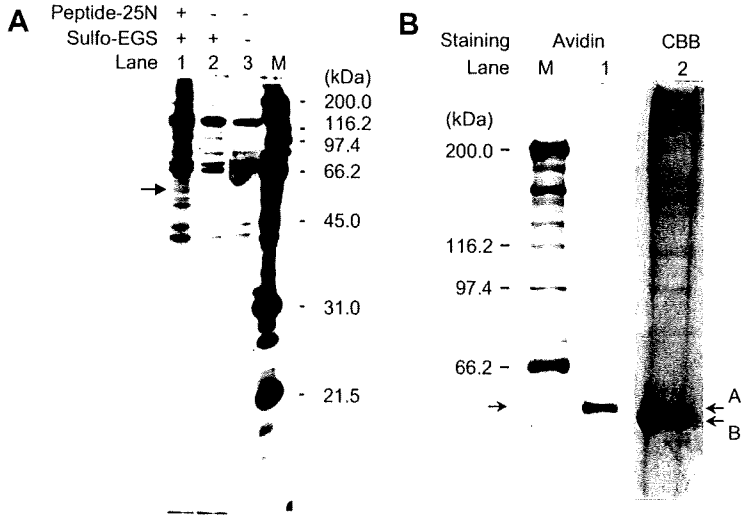

Fig. 1. Detection and purification of the target molecule of Peptide-25N. (A) Membrane fraction of BAEC was applied to SDS–PAGE with avidin staining and the candidate of the target molecule of Peptide-25N was detected (an arrow). (B) The target molecule fraction was obtained from the avidin–biotin affinity chromatography and applied onto SDS–PAGE followed by avidin (lane 1) or CBB staining (lane 2). Arrow A indicates the putative complex containing biotinylated Peptide-25N and arrow B does the co-eluted protein.

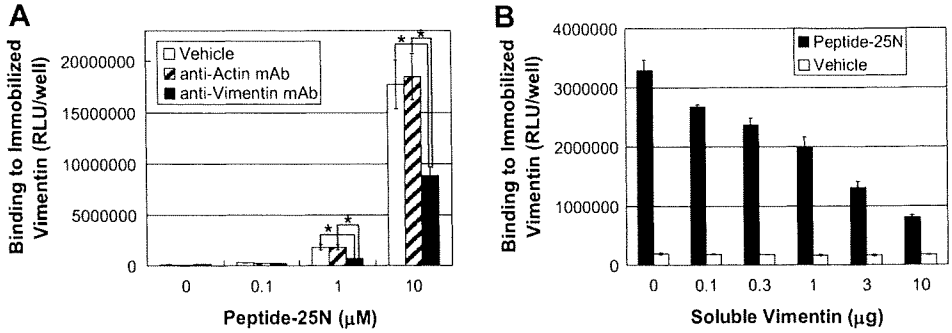

Fig. 3. Specific binding of Peptide-25N to immobilized vimentin protein. (A) Binding of Peptide-25N to immobilized vimentin protein was verified by adding anti-vimentin mAb clone VIM3B, unrelated anti-α-actin mAb clone ASM-1 or vehicle. The data are shown as the mean and S.D. from four samples. $^{*}P < 0.005$. (B) Binding of Peptide-25N to immobilized vimentin protein was investigated by adding soluble vimentin. Background of the system is also shown. The data are shown as the mean and S.D. from four samples.

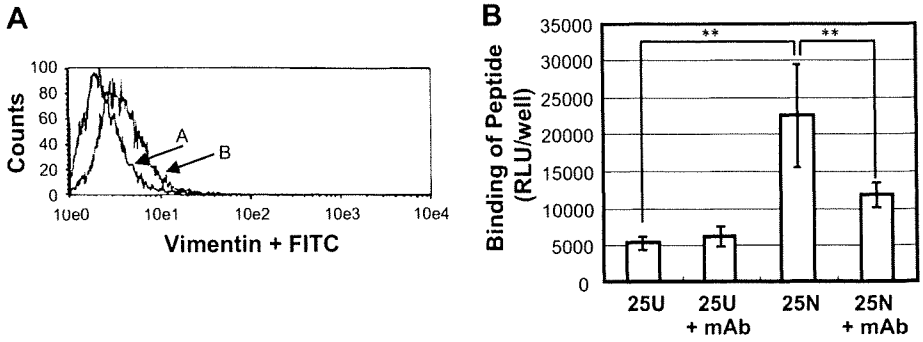

Fig. 4. Contribution of vimentin in binding of Peptide-25 to cell surface of BAECs. (A) The expression of vimentin on cell surface of BAECs was analyzed by FACS. A, Mouse IgG2a as a negative control; B, anti-vimentin mAb (VIM3B4). The intensity of VIM3B4 (B) was significantly higher than that of control (A) ($P < 0.001$). (B) Binding of biotin-labeled (25N) or unlabeled (25U) peptide to BAECs was measured as described in Section 2. In some experiments, anti-vimentin mAb (VIM3B4) was added. The data are shown as the mean and S.D. of eight samples. $^{**}P < 0.01$.

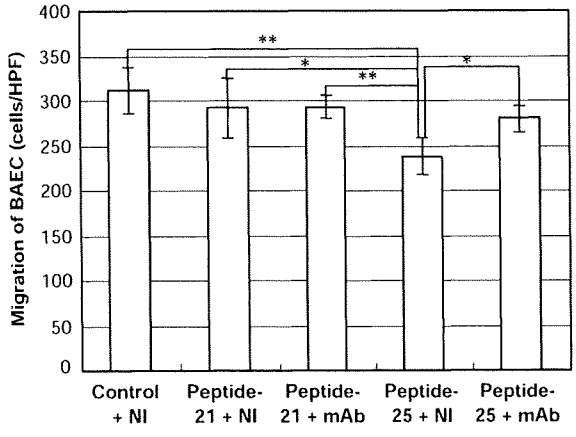

Fig. 5. Contribution of vimentin in LTGF-β activation by Peptide-25. To detect activity of TGF-β, migration assay was performed in the presence of Peptide-25 or Peptide-21 (negative control) as described in Section 2. In some experiments anti-vimentin mAb or mouse IgG1 as a negative control was added. The data are shown as the mean and SD of four samples. $^{*}P < 0.05$ and $^{**}P < 0.01$.

Glu113 to Arg131 in the LAP molecule) could not augment LTGF-β binding to cells and activation [9]. Therefore, we concluded that vimentin is involved in the latent TGF-β activation by Peptide-25.

4. Discussion

Vimentin is one of the cytoskeletal proteins classified as an intermediate filament. However, vimentin is secreted by activated macrophages in response to inflammatory signals for efficient killing of microorganisms [13], suggesting the involvement of vimentin in immune function. Macrophages are thought to be the principle source of TGF-β during inflammatory response [14] and active TGF-β is thought to be involved in various inflamed diseases such as rheumatoid arthritis [15]. One of the mechanisms of LTGF-β activation is partial enzymatic cleavage or degradation of LTGF-β by such as plasmin, matrix metalloprotease, and calpain [5,6,8] and the inflamed diseases show the elevated activity of those cell-associated proteases [5,16]. We speculate the mechanism of LTGF-β activation by the LAP fragments as following: (1) degradation of LAP by elevated proteolysis on cell surface generates LAP fragments, (2) active TGF-β is released from latent complex and exerts its activities, (3) the LAP fragments bind to vimentin on cell surface, (4) binding of LTGF-β to the cell surface is augmented by the LAP fragment, and (5) the additional activation occurs. To our knowledge, this is the first report indicating that vimentin is involved in the LTGF-β activation mechanism. The precise mechanisms remain to be elucidated how the LAP fragments and vimentin can work together to draw the LTGF-β complex to the cell surface. It is critical to control the excessive activation of LTGF-β for the treatment. We expect to develop a new type of TGF-β inhibitors through the study of activation of LTGF-β.

References

[1] Annes, J.P., Munger, J.S. and Rifkin, D.B. (2003) Making sense of latent TGFβ activation. J. Cell Sci. 116, 217–224.

[2] Ahamed, J., Burg, N., Yoshinaga, K., Janczak, C.A., Rifkin, D.B. and Coller, B.S. (2008) In vitro and in vivo evidence for shear-induced activation of latent transforming growth factor-β1. Blood 112, 3650–3660.

[3] Young, G.D. and Murphy-Ullrich, J.E. (2004) The tryptophan-rich motifs of the thrombospondin type 1 repeats bind VLAL motifs in the latent transforming growth factor-β complex. J. Biol. Chem. 279, 47633–47642.

[4] Annes, J.P., Chen, Y., Munger, J.S. and Rifkin, D.B. (2004) Integrin $\alpha_v\beta_6$-mediated activation of latent TGF-β binding protein-1. J. Cell Biol. 165, 723–734.

[5] Jakins, G. (2008) The role of proteases in transforming growth factor-β activation. Int. J. Biochem. Cell. Biol. 40, 1068–1078.

[6] Sato, Y. and Rifkin, D.B. (1989) Inhibition of endothelial cell movement by pericytes and smooth muscle cells: Activation of a latent transforming growth factor-β1 molecule by plasmin during co-culture J. Cell Biol. 109, 309–315.

[7] Sato, Y., Okada, F., Abe, M., Seguchi, T., Kuwano, M., Sato, S., Furuya, A., Hanai, N. and Tamaoki, T. (1993) The mechanism for the activation of latent TGF-β during co-culture of endothelial cells and smooth muscle cells: Cell-type specific targeting of latent TGF-β to smooth muscle cells. J. Cell Biol. 123, 1249–1254.

[8] Abe, M., Oda, N. and Sato, Y. (1998) Cell-associated activation of latent transforming growth factor-β by calpain. J. Cell. Physiol. 174, 186–193.

[9] Abe, M., Oda, N., Sato, Y., Shibata, K. and Yamasaki, M. (2002) Augmented binding and activation of latent transforming growth factor-β by a tryptic fragment of latency associated peptide. Endothelium 9, 25–36.

[10] Clement, S., Velasco, P.T., Murthy, S.N.P., Wilson, J.H., Lukas, T.J., Goldman, R.D. and Lorand, L. (1998) The intermediate filament protein, vimentin, in the lens is a target for cross-linking by transglutaminase. J. Biol. Chem. 273, 7604–7609.

[11] Kojima, S., Vernooy, R., Moscatelli, D., Amanuma, H. and Rifkin, D.B. (1995) Lipopolysaccharide inhibits activation of latent transforming growth factor-β in bovine endothelial cells. J. Cell. Physiol. 163, 210–219.

[12] Kalo, E., Buganim, Y., Shapira, K.E., Besserglick, H., Goldfinger, N., Weisz, L., Stambolsky, P., Heins, Y.I. and Rotter, V. (2007) Mutant p53 attenuates the SMAD-dependent transforming growth factor β1 (TGF-β1) signaling pathway by repressing the expression of TGF-β receptor type II. Mol. Cell. Biol. 27, 8228–8242.

[13] Mor-Vankin, N., Punturieri, A., Sitwala, K. and Markovitz, D.M. (2003) Vimentin is secreted by activated macrophages. Nat. Cell Biol. 5, 59–63.

[14] Wahl, S., McCartney-Francis, N., Allen, J.B., Dougherty, E.B. and Dougherty, S.F. (1990) Macrophage production of TGF-β and regulation of TGF-β. Ann. NY Acad. Sci. 593, 188–196.

[15] Lettesjo, H., Nordstrom, E., Strom, H., Nilsson, B., Glinghammar, B., Dahlstedt, L. and Moller, E. (1998) Synovial fluid cytokines in patients with rheumatoid arthritis or other arthritic lesions. Scand. J. Immunol. 48, 286–292.

[16] Fukui, I., Tanaka, K. and Murachi, T. (1989) Extracellular appearance of calpain and calpastatin in the synovial fluid of the knee joint. Biochem. Biophys. Res. Commun. 162, 559–566.

Hypertension
JOURNAL OF THE AMERICAN HEART ASSOCIATION

Effect of Recombinant Placental Growth Factor 2 on Hypertension Induced by Full-Length Mouse Soluble fms-Like Tyrosine Kinase 1 Adenoviral Vector in Pregnant Mice

Hirotada Suzuki, Akihide Ohkuchi, Shigeki Matsubara, Yuji Takei, Masato Murakami, Masabumi Shibuya, Mitsuaki Suzuki and Yasufumi Sato

Hypertension 2009;54;1129-1135; originally published online Sep 28, 2009;
DOI: 10.1161/HYPERTENSIONAHA.109.134668
Hypertension is published by the American Heart Association. 7272 Greenville Avenue, Dallas, TX 72514
 Print ISSN: 0194-911X. Online ISSN: 1524-4563

Effect of Recombinant Placental Growth Factor 2 on Hypertension Induced by Full-Length Mouse Soluble fms-Like Tyrosine Kinase 1 Adenoviral Vector in Pregnant Mice

Hirotada Suzuki, Akihide Ohkuchi, Shigeki Matsubara, Yuji Takei, Masato Murakami, Masabumi Shibuya, Mitsuaki Suzuki, Yasufumi Sato

Abstract—The first aim of our study was to develop a pregnant mouse model for preeclampsia using adenoviral vector containing mouse full-length soluble fms-like tyrosine kinase 1 (sFlt-1) but not truncated sFlt-1. The second aim was to evaluate effects of recombinant mouse (rm) vascular endothelial growth factor (VEGF) and rm placental growth factor (PlGF) on a preeclampsia model induced by adenoviral vector containing mouse full-length sFlt-1. We injected adenoviral vector containing mouse full-length sFlt-1 on day 8.5 or 9.5 of gestation into pregnant Institute of Cancer Research mice, resulting in hypertension, proteinuria, and similar glomerular histological changes as those seen in human preeclamptic women with glomerular endotheliosis on day 16.5 or 17.5 of gestation. The preeclampsia models were treated with 100 μg/kg of rmVEGF164 (n=5), 100 μg/kg of rmPlGF-2 (n=5), or vehicle (n=7) twice a day for 2 days IP. The rmVEGF164 treatment significantly decreased the mean blood pressure on day 16.5 or 17.5 of gestation compared with the vehicle treatment (85±4 versus 97±2 mm Hg; P=0.018). The rmPlGF-2 treatment also significantly decreased the mean blood pressure on day 16.5 or 17.5 of gestation compared with the vehicle treatment (86±3 versus 97±2 mm Hg; P=0.018). However, proteinuria was not affected by either rmVEGF164 or rmPlGF-2. In conclusion, we, for the first time, created a mouse preeclampsia model using mouse full-length sFlt-1. VEGF and PlGF may be promising for ameliorating hypertension in women with preeclampsia. Additional study of PlGF as a potential drug for preeclampsia is warranted. (***Hypertension.* 2009;54:1129-1135.**)

Key Words: adenoviral vector ■ soluble fms-like tyrosine kinase 1 ■ vascular endothelial growth factor ■ placental growth factor ■ preeclampsia ■ animal models ■ therapy

Preeclampsia is associated with maternal and infantile morbidity and mortality.[1,2] It has been shown that the concentration of soluble fms-like tyrosine kinase 1 (sFlt-1), a circulating antiangiogenic protein, is increased in women with preeclampsia,[3,4] and increased levels of sFlt-1 and reduced levels of free placental growth factor (PlGF) are potentially useful for predicting the subsequent development of preeclampsia.[4,5] SFlt-1 acts by adhering to the receptor-binding domains of vascular endothelial growth factor (VEGF)-A and PlGF, preventing their interaction with endothelial receptors on the cell surface. Recent studies have indicated that patients with cancer receiving anti-VEGF antibody therapy may have an increased incidence of proteinuria and hypertension because of a decrease in their circulating VEGF levels.[6] Nonpregnant and pregnant rodents administered anti-VEGF antibodies or sFlt-1 manifested proteinuria and hypertension.[3,7,8] These results strongly indicate that increases in sFlt-1 and decreases in VEGF/PlGF in the maternal circulation may cause the occurrence of preeclampsia.

SFlt-1, a human natural soluble form of the VEGF receptor (VEGFR) 1, is produced in conditioned culture medium of human umbilical vein endothelial cells[9] and in the trophoblasts.[10,11] SFlt-1 is encoded by the flt-1 gene and is truncated between N-terminal immunoglobulin-like domains 6 and 7.[12] Because the N-terminal first and second domains of Flt-1 are necessary and sufficient for the binding of VEGF-A with near-native affinity,[13,14] truncated sFlt-1$^{1-3}$ containing the first to third domains, but not full-length sFlt-1, has been used for the studies evaluating the effect of sFlt-1 on hypertension and proteinuria in mouse or rat models.[3,7,15–19] However, there are 2 differences between the full-length sFlt-1 and truncated sFlt-1$^{1-3}$: first, the full-length sFlt-1 has a 31-amino acid carboxyl lesion derived from an intron, which is significantly homologous to that in mammals,[11] and, second, the truncated sFlt-1$^{1-3}$ lacks the immunoglobulin-like loop 4, which is essential to stabilize receptor dimerization of the extracellular domains of Flt-1, in addition to VEGF.[13,14] Therefore, the effect of sFlt-1 on the occurrence of hyperten-

Received April 27, 2009; first decision May 17, 2009; revision accepted September 1, 2009.

From the Department of Obstetrics and Gynecology (H.S., A.O., S.M., Y.T., M.Su.), Jichi Medical University School of Medicine, Tochigi, Japan; Division of Genetics (M.M., M.Sh.), Institute of Medical Science, University of Tokyo, Tokyo, Japan; Institute of Development, Aging, and Cancer (Y.S.), Department of Vascular Biology, University of Tohoku, Sendai, Japan.

Correspondence to Akihide Ohkuchi, Department of Obstetrics and Gynecology, Jichi Medical University School of Medicine, 3311-1 Yakushiji, Shimotsuke-shi, Tochigi 329-0498, Japan. E-mail okuchi@jichi.ac.jp

Hypertension is available at http://hyper.ahajournals.org DOI: 10.1161/HYPERTENSIONAHA.109.134668

sion or proteinuria may be different between truncated sFlt-1 and natural full-length sFlt-1.

It has been reported that the effect of excess circulating sFlt-1 can be ameliorated by the administration of recombinant VEGF-A.[7-19] However, in humans, a decrease in PlGF is related to the later occurrence of preeclampsia.[20-22] Therefore, we also hypothesized that not only VEGF-A, but also PlGF, may play a pivotal role in the occurrence of hypertension and proteinuria in both humans and rodents. To our knowledge, the effect of the administration of PlGF into a rodent model of preeclampsia via a mouse (m)-sFlt-1 adenoviral vector has not been examined.

First, we evaluated an adenovirus encoding the full-length mouse-sFlt-1 gene (Ad m-sFlt-1) for the induction of hypertension and proteinuria in pregnant mice. Second, we evaluated the effects of recombinant mouse (rm) VEGF164 (rmVEGF164) and rmPlGF-2 on hypertension and proteinuria in a mouse preeclampsia model induced by Ad m-sFlt-1.

Methods

An expanded Materials and Methods section is available in the online Data Supplement (available at http://hyper.ahajounals.org). Briefly, in the first experiment, an Ad m-sFlt-1, which was created in our previous study,[23] and an adenovirus encoding β-galactosidase gene (Ad LacZ) were propagated in HEK293cells. The viral lysates were purified and concentrated through 2 cycles of CsCl step gradients.[24] Nine- to 12-week-old CD1 (Institute of Cancer Research) mice were injected in the tail vein with 3×10^8 plaque-forming unit (PFUs; low dose), 1×10^9 PFUs (medium dose), or 2×10^9 PFUs (high dose) of Ad m-sFlt-1 (n=9, n=6, and n=6, respectively) and with 3×10^8 PFUs (low dose), 1×10^9 PFUs (medium dose), or 2×10^9 PFUs (high dose) of Ad LacZ (n=7, n=6, and n=7, respectively) on day 8.5 or 9.5 of gestation. The control pregnancy mice were not injected with anything (n=7). The mean blood pressures (MBPs) were measured by the tail-cuff method (Softron Ltd) on 4 different days: (1) before mating, (2) just before the injection of adenovirus, (3) on day 13.5 or 14.5 of gestation, and (4) on day 16.5 or 17.5 of gestation. The urine albumin:creatinine (Alb/Cre) ratios on day 16.5 or 17.5 of gestation were measured. In the second experiment, pregnant mice were injected in their tail vein with 2×10^9 PFUs (high dose) of Ad m-sFlt-1 on day 8.5 or 9.5 of gestation. rmVEGF164 (100 μg/kg diluted in 500 μL of PBS; n=5) was administered IP twice a day for 2 days from the evening on day 14.5 or 15.5 of gestation. In other mice, rmPlGF-2 (100 μg/kg diluted in 500 μL of PBS; n=5) and the vehicle (500 μL of PBS; n=7) were administered IP twice a day for 2 days. The MBP and Alb/Cre ratio were also measured. All of the animal housing and experiments were approved by the institutional animal care and research advisory committee of both the University of Tohoku and Jichi Medical University. The pharmacokinetics of rmVEGF164 and rmPlGF-2 in nonpregnant mice and pregnant mice are shown in the online Data Supplement (available at http://hyper.ahajournals.org, Figure S1A through S1D).

Results

Expression of Proteins by the Adenoviral Vector

In mice administered Ad LacZ, β-galactosidase activity was observed in the liver but not in the placenta by 5-bromo-4-chloro-3-indolyl β-D-galactoside staining, suggesting that Ad m-sFlt-1 was expressed in the liver. The levels of mouse sFlt-1 (nanograms per milliliter) on day 16.5 or 17.5 of gestation increased significantly in the medium and high doses of Ad m-sFlt-1 compared with the medium and high doses of Ad LacZ, respectively (85 [58 to 95] versus, 12 [12 to 29], $P=0.002$; 93 [82 to 130] versus 25 [21 to 33], $P=0.001$, respectively; Figure 1A). The levels of mouse sFlt-1 on day 16.5 or 17.5 of gestation were not different among the control and the mice administered the low, medium, and high dose of Ad LacZ ($P=0.76$ by Kruskal-Wallis test).

Plasma Levels of Angiogenic Factors in Mice Administered Ad m-sFlt-1

The plasma levels of mouse VEGF-A (picograms per milliliter) on day 16.5 or 17.5 of gestation in the mice administered high-dose Ad m-sFlt-1 were significantly lower than in the mice administered high dose Ad LacZ (47 [43 to 52] versus 95 [93 to 113]; $P=0.001$; Figure 1B). On the contrary, the levels of mouse PlGF-2 (picograms per milliliter) on day 16.5 or 17.5 of gestation were almost the same among the control mice, the high-dose Ad LacZ group, and the high-dose Ad m-sFlt-1 group (21 [14 to 26], 25 [21 to 35], and 30 [23 to 38]; Figure 1C).

Blood Pressure and Proteinuria in Pregnant Mice Administered Ad m-sFlt-1

In the control mice and the mice administered low, medium, and high doses of Ad LacZ, MBP (millimeters of mercury) was almost the same during the prepregnancy period and during pregnancy (Figure 1D). In the mice administered high-dose Ad m-sFlt-1, MBP was significantly increased between day 8.5 or 9.5 and day 13.5 or 14.5 (76±2 versus 91±4; $P=0.028$) and between day 13.5 or 14.5 and day 16.5 or 17.5 (91±4 versus 101±3; $P=0.028$), although such increases were not seen in the mice administered low or medium doses of Ad m-sFlt-1 (Figure 1E). The MBP on day 16.5 or 17.5 of gestation in the high-dose Ad m-sFlt-1 group was significantly higher than that in the high-dose Ad LacZ group (101±3 versus 81±11; $P=0.010$) and the control group (83±4; $P=0.005$). The urine Alb/Cre ratios (milligrams per gram) on day 16.5 or 17.5 of gestation in the mice administered low, medium, and high doses of Ad m-sFlt-1 were significantly increased compared with those in the mice administered low, medium, and high doses of Ad LacZ, respectively (5.8 [4.5 to 14] versus 2.7 [2.4 to 2.9], $P=0.030$; 92 [43 to 148] versus 10 [4.9 to 22], $P=0.015$; 58 [30 to 161] versus 5.2 [4.0 to 13], $P=0.020$, respectively), although the urine Alb/Cre ratio in the low-dose Ad m-sFlt-1 group was not significantly different from that in the control mice (8.3 [3.6 to 11]; Figure 1F).

Histopathology in Mice Administered Ad m-sFlt-1

Glomerular histologies viewed by light microscopy in mice administered high-dose Ad m-sFlt-1 (Figure S2D and S2E) and those in the mice administered high-dose Ad LacZ (Figure S2A and S2B), scanning electron microscopy of glomerulus in mice administered high-dose Ad m-sFlt-1 and Ad Lac Z (Figure S2F and S2C), and the mean fetal and placental weights among the control mice, the high-dose Ad LacZ group, and the high-dose Ad m-sFlt-1 group (Figure S2G and S2H) were shown in the online Data Supplement. These results were written in the online Data Supplement.

Relationship Among the Plasma Levels of Mouse sFlt-1, Mouse VEGF-A, Blood Pressure, and Proteinuria

Among all of the data in control mice, mice administered Ad LacZ, and mice administered Ad m-sFlt-1, there was an

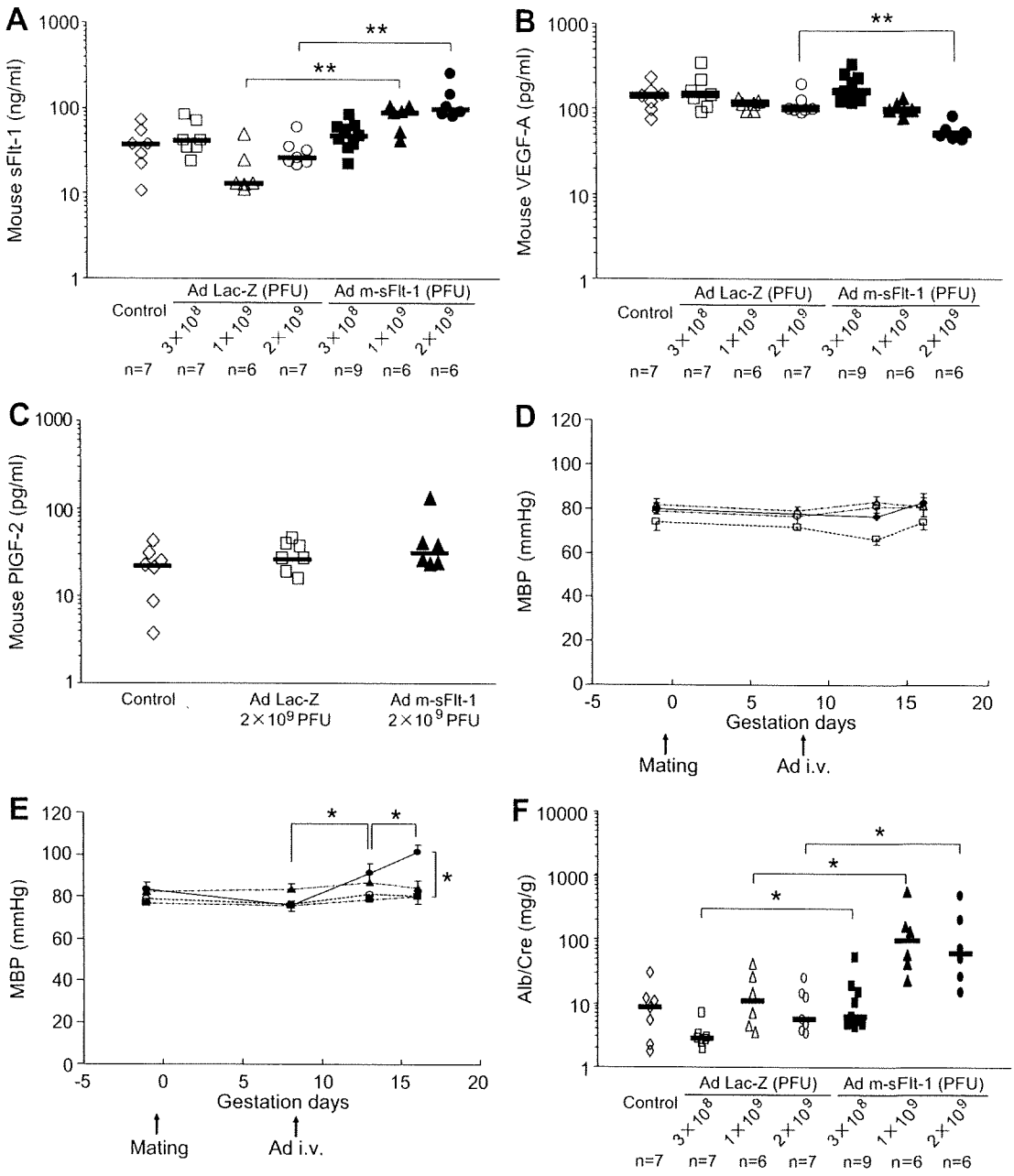

Figure 1. Data from pregnant mice administered nothing, Ad LacZ, and Ad m-sFlt-1. A, Plasma levels of m-sFlt-1 on day 16.5 or 17.5 of gestation. B, Plasma levels of m-VEGF-A (picograms per milliliter) on day 16.5 or 17.5 of gestation. C, Plasma levels of m-PlGF-2 (picograms per milliliter) on day 16.5 or 17.5 of gestation. D, MBP (millimeters of mercury) during the prepregnancy period, on day 8.5 or 9.5 of gestation, on day 13.5 or 14.5 of gestation, and on day 16.5 or 17.5 of gestation. ♦, □, △, and ○ represent the values in the control pregnant mice and pregnant mice administered low-dose (3×10^8 PFU), medium-dose (1×10^9 PFU), and high-dose (2×10^9 PFU) Ad LacZ, respectively. E, MBP (millimeters of mercury) during the prepregnancy period, on day 8.5 or 9.5 of gestation, on day 13.5 or 14.5 of gestation, and on day 16.5 or 17.5 of gestation. ○, ■, ▲, and ● represent the values in pregnant mice administered high-dose Ad LacZ and mice administered low-dose, medium-dose, and high-dose Ad m-sFlt-1, respectively. F, Urine Alb/Cre ratios (milligrams per gram) on day 16.5 or 17.5 of gestation. $^*P<0.05$; $^{**}P<0.01$.

inverse relationship between the plasma levels of log10sFlt-1 and log10VEGF-A ($r=-0.29$; $P=0.042$; Figure 2A); positive relationships between the plasma levels of log10sFlt-1 and MBP ($r=0.24$; $P=0.098$; Figure 2B) and between the plasma levels of log10sFlt-1 and urine log10(Alb/Cre; $r=0.44$; $P=0.002$; Figure 2C); and inverse relationships between the plasma levels of log10VEGF-A and MBP ($r=-0.33$; $P=0.023$; Figure 2D) and between the plasma levels of log10VEGF-A and urine log10(Alb/Cre; $r=-0.44$; $P=0.002$; Figure 2E). Thus, the circulating levels of sFlt-1 are significantly positively related to the degree of proteinuria, whereas the circulating levels of VEGF-A are significantly inversely related to both blood pressure and proteinuria. Our results indicate that decreased levels of circulating VEGF-A cause the increases in blood pressure seen in the mice administered Ad m-sFlt-1.

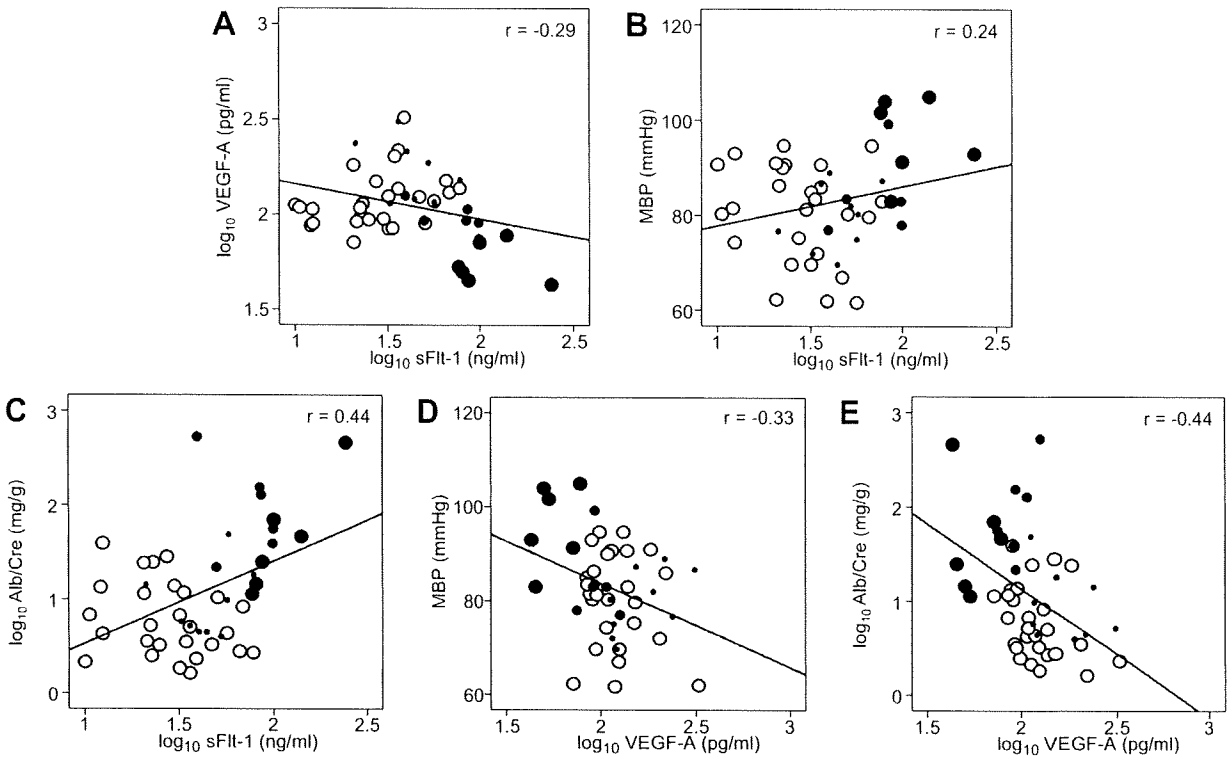

Figure 2. Scattergrams showing the relationship between the plasma levels of log10sFlt-1 and log10VEGF-A (A; $r=-0.29$; $P=0.042$), between the plasma levels of log10sFlt-1 and MBP (B; $r=0.24$; $P=0.098$), between the plasma levels of log10sFlt-1 and urine log10(Alb/Cre) (C; $r=0.44$; $P=0.002$), between the plasma levels of log10VEGF-A and MBP (D; $r=0.33$; $P=0.023$), and between the plasma levels of log10VEGF-A and urine log10(Alb/Cre) (E; $r=-0.44$; $P=0.002$). The large open circles represent combined data from the control mice and mice administered low, medium, and high doses of Ad LacZ. The small, medium, and large closed circles represent data from mice administered low, medium, and high doses of Ad m-sFlt-1, respectively.

Effects of rmVEGF164 and rmPlGF-2 in Mice Administered High-Dose Ad m-sFlt-1

In pregnant mice administered high-dose Ad m-sFlt-1 compared with mice administered vehicle, the levels of mouse VEGF-A (pg/ml) 3 to 4 hours after the last administration of rmVEGF164 were significantly increased (356 [121 to 793] versus 59 [56 to 68]; $P=0.010$; Figure 3A), and the level of mouse PlGF-2 (pg/ml) 3 to 4 hours after the last administration of rmPlGF-2 was also significantly increased (244 [133 to 244] versus 60 [52 to 74]; $P=0.010$; Figure 3B).

The rmVEGF164 treatment significantly decreased the MBP (mm Hg) on day 16.5 or 17.5 of gestation compared with the vehicle treatment (85±4 versus 97±2; $P=0.018$; Figure 3C). The rmPlGF-2 treatment also significantly decreased the MBP on day 16.5 or 17.5 of gestation compared with the vehicle treatment (86±3 versus 97±2; $P=0.018$). However, the urine Alb/Cre levels were not affected by treatment with either rmVEGF164 or rmPlGF-2 (Figure 3D). The rmVEGF164 treatment and rmPlGF-2 treatment did not ameliorate glomerular histology viewed by light microscopy in pregnant mice administered high-dose Ad m-sFlt-1 compared with those administered vehicle.

Discussion

In this study, we created a pregnant mouse model of preeclampsia, showing hypertension, proteinuria, and glomerular change, like endotheliosis, by transfecting a high dose (2×10^9 PFUs) of adenovirus encoding full-length m-sFlt-1. In addition, we revealed that rmVEGF164 and rmPlGF-2 ameliorate the hypertension induced by the administration of a high dose of Ad m-sFlt-1 in pregnant mice.

Development of a Pregnant Mouse Model of Preeclampsia Using Ad m-sFlt-1 and the Relationships Between the Serum Levels of m-sFlt-1/m-VEGF-A/m-PlGF-2 and Hypertension/Proteinuria

We, for the first time, created a mouse preeclampsia model using full-length m-sFlt-1 instead of truncated m-sFlt-1, which has been used in previous mouse preeclampsia models.[3,7,15–19] In the previous rat models using truncated m-sFlt-1, both hypertension and proteinuria emerged after low-dose (1×10^8-PFU) administration of Ad m-sFlt-1.[3] On the contrary, we needed a higher dose of Ad m-sFlt-1 to generate both hypertension and proteinuria. In our study, increases in the plasma levels of sFlt-1 were related to the occurrence of proteinuria, and decreases in the plasma levels of VEGF-A were related to the occurrence of both hypertension and proteinuria. Therefore, the circulating levels of sFlt-1 and VEGF-A may be important for the occurrence of hypertension and proteinuria. It is possible that the in vivo expression of sFlt-1 in the liver per administered dose of adenovirus or the circulating levels of sFlt-1 or VEGF-A were different between the 2 studies.

It is well known that the administration of sFlt-1 into rodents results in the occurrence of proteinuria.[3,7,16,25] Kamba

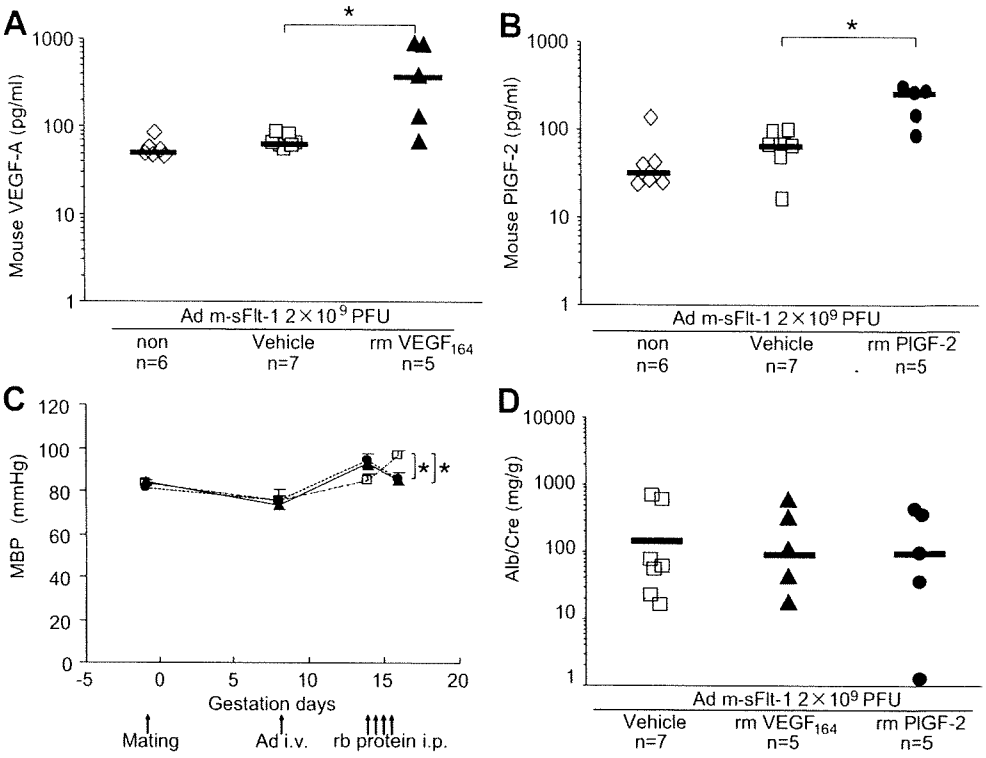

Figure 3. Data in pregnant mice administered high-dose Ad m-sFlt-1 after treatment with vehicle, rmVEGF164, or rmPlGF-2. A, The levels of mouse VEGF-A 3 to 4 hours after the last administration of nothing, vehicle (twice a day, 4 times), or rmVEGF164 (100 μg/kg, twice a day, 4 times). B, The levels of mouse PlGF-2 3 to 4 hours after the last administration of nothing, vehicle (twice a day, 4 times), or rmPlGF-2 (100 μg/kg, twice a day, 4 times). C, MBP (millimeters of mercury) during the prepregnancy period, just before the injection of Ad m-sFlt-1, just before the administration of recombinant proteins or vehicle, and at 1 to 2 hours after the last administration of recombinant proteins or vehicle. □, ▲, and ● represent the values in pregnant mice administered a high dose of Ad m-sFlt-1 with vehicle (n=7), rmVEGF164 (n=5), or rmPlGF-2 (n=5), respectively. D, Urine Alb/Cre ratios on day 16.5 or 17.5 of gestation in pregnant mice administered a high dose of Ad m-sFlt-1 with vehicle, rmVEGF164, or rmPlGF-2. *$P<0.05$.

et al[25] reported that proteinuria, but not hypertension, emerged in nonpregnant mice administered adenovirus-truncated m-sFlt-1. Sugimoto et al[7] reported that IV administration of an sFlt-1/Fc chimera protein into nonpregnant mice resulted in proteinuria 3 hours after the administration. Maynard et al[3] reported that IV administration of adenovirus-truncated m-sFlt-1 into nonpregnant and pregnant rats resulted in severe proteinuria. In addition, the effect of adenovirus-truncated m-sFlt-1 in pregnant rats on the occurrence of proteinuria was more severe than that of adenovirus-soluble endoglin, both of which can cause both hypertension and proteinuria in pregnant mice.[16] However, the proteinuria presented in this mouse model is fairly modest compared with what is presented in the rats where the Alb/Cre ratio is frequently $\geq$1000 mg/g.[3] One possibility is that the dose using the full-length sFlt1 is not enough, because it tends to have a poor bioavailability in contrast to truncated sFlt1. Another possibility is that proteinuria may depend on the background of the mouse strains used.

In our experiment, the decrease in the circulating levels of VEGF-A, but not PlGF-2, was related to the increase in MBP. The effect of VEGF-A on blood pressure has been reported in humans.[26–29] The blocking of signal transduction of VEGF-A by anti-VEGF monoclonal antibody[26,27] and tyrosine kinase inhibitors, such as soraferib[28] and sumitinib,[29] induces hypertension. On the contrary, the administration of rmVEGF-A results in a decrease of MBP in rats.[30,31] Thus, an appropriate circulating VEGF-A level appears to be important for the maintenance of normal blood pressure. Although the detailed mechanism by which a decreased level of VEGF-A affects the occurrence of hypertension has not been elucidated, the modulation of the production of NO by VEGF-A via endothelial NO synthase activity in endothelial cells may be related to the change in blood pressure.[32,33]

The mouse PlGF-2 was not altered in this mouse model of preeclampsia. The circulating levels of PlGF-1 are low in preeclamptic women,[3–5,19–21] because the human ELISA assay measured free PlGF but not total PlGF. We could not know whether the assay of the mouse PlGF-2 in our study measured a free or total PlGF-2 assay. We speculate that the assay of the mouse VEGF-A measured a free VEGF-A and that the assay of the mouse PlGF-2 measured a total PlGF-2, because the levels of VEGF-A were decreased but the levels of PlGF-2 were not decreased by the administration of high-dose Ad m-sFlt-1.

Effect of rmVEGF164 and rmPlGF-2 on Blood Pressure and Proteinuria in a Pregnant Mouse Preeclampsia Model

We revealed that rmVEGF164 ameliorates the hypertension induced by the administration of a high dose of Ad m-sFlt-1

in pregnant mice. Li et al[19] reported the therapeutic effect of VEGF-A in preeclamptic rat models induced by the IV administration of truncated Ad m-sFlt-1 on 8 days of gestation; the SC administration of 800 μg/kg per day of recombinant human VEGF121 for 6 days during day 11 to day 16 of gestation resulted in the amelioration of systolic blood pressure. In our study, the administered doses of rmVEGF164 were lower, and the treatment duration of rmVEGF164 was shorter compared with the study of Li et al[19]; however, the MBP after the administration of rmVEGF164 decreased. Therefore, the administration of recombinant VEGF-A to women with preeclampsia may be an effective treatment for this condition, especially for women with early onset preeclampsia, in whom the delay of birth by weeks may contribute to the reduction of neonatal complications and neonatal stay in the newborn intensive care unit.[34]

We, for the first time, revealed that rmPlGF-2 ameliorates the hypertension induced by high doses of Ad m-sFlt-1 in pregnant mice. To the best of our knowledge, this is the first experiment that showed the antihypertensive effect of rmPlGF on the hypertension induced by Ad m-sFlt-1 in pregnant mice. Hypotension induced by VEGF-A is mainly mediated by VEGFR2.[30] Because PlGF binds only to VEGFR1 and has little or no direct mitogenic or permeability-enhancing activity,[35,36] we supposed that the hypotensive effect of PlGF is very weak. However, surprisingly, the antihypertensive effect of PlGF was as strong as the antihypertensive effect of VEGF-A in our preeclampsia mouse model. Recently, Osol et al[37] reported that PlGF had a vasodilatory effect on numerous arteries and veins in rats; pregnancy significantly enhanced sensitivity to PlGF in rat uterine arteries; the vasodilatory effect of PlGF during pregnancy was mainly attributed to the activation of VEGFR1 but not VEGFR2; VEGFR1 was upregulated in the uterine artery wall during gestation; and PlGF dilation was principally mediated by the release of NO in rat uterine arteries. In addition, Osol et al[37] also showed that both rat mesenteric and human SC arteries dilated in response to PlGF in an NO-independent manner. These observations clearly suggest that PlGF has the ability to dilate vessels during pregnancy; that is, PlGF has a potentially antihypertensive effect during pregnancy.

Possible Mechanism by Which Hypertension and Proteinuria Emerge in a Pregnant Mouse Administered Recombinant sFlt-1

Recently, Bridges et al[8] reported that placental and vascular superoxide productions were increased and plasma VEGF-A concentrations were decreased in pregnant rats administered recombinant sFlt-1 chronically during days 13 to 18 of gestation. Vasorelaxations to both acetylcholine and sodium nitroprusside were decreased in pregnant rats administered recombinant sFlt-1, and the decrease of vasorelaxation to acetylcholine was attenuated by the addition of the superoxide scavenger Tiron, indicating elevated maternal sFlt-1, via the decrease of VEGF, results in increased oxidative stress that contributes to vascular dysfunction during pregnancy.[8] VEGF contributes to the maintenance of an appropriate balance of pro-oxidant and antioxidant factors via manganese superoxide dismutase[38] and NADPH oxidase,[39] and regulates NO production.[32,33] We also observed that the plasma VEGF levels were decreased in pregnant mice administered high doses of Ad m-sFlt-1 and the treatment of VEGF ameliorated hypertension induced by Ad m-sFlt-1. Therefore, increased oxidative stress and vascular dysfunction might be factors in hypertension in the present model, although we did not measure the oxidative stress. Taken together, VEGF antagonism may induce endothelial cell oxidative stress and contribute to renal dysfunction and hypertension.

Conclusions

We, for the first time, created a mouse preeclampsia model using full-length m-sFlt-1 instead of truncated m-sFlt-1, which has been used in previous mouse preeclampsia models.[3,7,15–19] Not only rmVEGF164, but also PlGF-2, ameliorated hypertension in the mouse preeclampsia model induce by full-length m-sFlt-1. Additional study of PlGF as a potential drug for preeclampsia is warranted.

Perspectives

Our study suggested a possible new therapy using PlGF for preeclamptic women. However, there are several unsolved issues. How many doses of PlGF-2 are sufficient for the amelioration of hypertension and proteinuria in the pregnant mouse model of preeclampsia using Ad m-sFlt-1? When should the administration of PlGF be started to restrict the occurrence of hypertension and proteinuria? What kinds of angiogenetic factors show the best therapeutic effects? In addition, if possible, we should make a mouse/rat model using adenoviral human sFlt-1, because the effect of m-sFlt-1 on mouse VEGF-A/PlGF might be different from that of human sFlt-1 on human VEGF-A/PlGF. If the human PlGF-1/PlGF-2 is used for the prevention/therapy of preeclampsia, we should carefully monitor the occurrence of possible adverse effects, such as lung edema, the development of new blood vessels in nontargeted tissues.

Sources of Funding

This work was funded by a Grant-in-Aid for Scientific Research from the Japan Society for the Promotion of Science (No. 18791169).

Disclosures

None.

References

1. Nagaya K, Fetters MD, Ishikawa M, Kubo T, Koyanagi T, Saito Y, Sameshima H, Sugimoto M, Takagi K, Chiba Y, Honda H, Mukubo M, Kawamura M, Satoh S, Neki R. Causes of maternal mortality in Japan. *JAMA*. 2000;283:2661–2667.
2. Hecher K, Campbell S, Doyle P, Harrington K, Nicolaides K. Assessment of fetal compromise by Doppler ultrasound investigation of the fetal circulation: arterial, intracardiac, and venous blood flow velocity studies. *Circulation*. 1995;91:129–138.
3. Maynard SE, Min JY, Merchan J, Lim KH, Li J, Mondal S, Libermann TA, Morgan JP, Sellke FW, Stillman IE, Epstein FH, Sukhatme VP, Karumanchi SA. Excess placental soluble fms-like tyrosine kinase 1 (sFlt1) may contribute to endothelial dysfunction, hypertension, and proteinuria in preeclampsia. *J Clin Invest*. 2003;111:649–658.
4. Levine RJ, Maynard SE, Qian C, Lim KH, England LJ, Yu KF, Schisterman EF, Thadhani R, Sachs BP, Epstein FH, Sibai BM, Sukhatme VP, Karumanchi SA. Circulating angiogenic factors and the risk of preeclampsia. *N Engl J Med*. 2004;350:672–683.

5. Levine RJ, Lam C, Qian C, Yu KF, Maynard SE, Sachs BP, Sibai BM, Epstein FH, Romero R, Thadhani R, Karumanchi SA; for the CPEP Study Group. Soluble endoglin and other circulating antiangiogenic factors in preeclampsia. *N Engl J Med*. 2006;355:992–1005.
6. Kabbinavar F, Hurwitz HI, Fehrenbacher L, Meropol NJ, Novotny WF, Lieberman G, Griffing S, Bergsland E. Phase II, randomized trial comparing bevacizumab plus fluorouracil (FU)/leucovorin (LV) with FU/LV alone in patients with metastatic colorectal cancer. *J Clin Oncol*. 2003; 21:60–65.
7. Sugimoto H, Hamano Y, Charytan D, Cosgrove D, Kieran M, Sudhakar A, Kalluri R. Neutralization of circulating vascular endothelial growth factor (VEGF) by anti-VEGF antibodies and soluble VEGF receptor 1 (sFlt-1) induces proteinuria. *J Biol Chem*. 2003;278:12605–12608.
8. Bridges JP, Gilbert JS, Colson D, Gilbert SA, Dukes MP, Ryan MJ, Granger JP. Oxidative stress contributes to soluble Fms-like tyrosine kinase-1 induced vascular dysfunction in pregnant rats. *Am J Hypertens*. 2009;22:564–568.
9. Kendall RL, Thomas KA. Inhibition of vascular endothelial cell growth factor activity by an endogenously encoded soluble receptor. *Proc Natl Acad Sci U S A*. 1993;90:10705–10709.
10. Clark DE, Smith SK, He Y, Day KA, Licence DR, Corps AN, Lammoglia R, Charnock-Jones DS. A vascular endothelial growth factor antagonist is produced by the human placenta and released into the maternal circulation. *Biol Reprod*. 1998;59:1540–1548.
11. Yamaguchi S, Iwata K, Shibuya M. Soluble Flt-1 (soluble VEGFR-1), a potent natural antiangiogenic molecule in mammals, is phylogenetically conserved in avians. *Biochem Biophys Res Commun*. 2002;291:554–559.
12. Chen H, Ikeda U, Shimpo M, Maeda Y, Shibuya M, Ozawa K, Shimada K. Inhibition of vascular endothelial growth factor activity by transfection with the soluble FLT-1 gene. *J Cardiovasc Pharmacol*. 2000;36: 498–502.
13. Barleon B, Totzke F, Herzog C, Blanke S, Kremmer E, Siemeister G, Marmé D, Martiny-Baron G. Mapping of the sites for ligand binding and receptor dimerization at the extracellular domain of the vascular endothelial growth factor FLT-1. *J Biol Chem*. 1997;272:10382–10388.
14. Shinkai A, Ito M, Anazawa H, Yamaguchi S, Shitarai K, Shibuya M. Mapping of the sites involved in ligand association and dissociation at the extracellular domain of the kinase insert domain-containing receptor for vascular endothelial growth factor. *J Biol Chem*. 1998;273:31283–31288.
15. Kuo CJ, Farnebo F, Yu EY, Christofferson R, Swearingen RA, Carter R, von Recum HA, Yuan J, Kamihara J, Flynn E, D'Amato R, Folkman J, Mulligan RC. Comparative evaluation of the antitumor activity of antiangiogenic proteins delivered by gene transfer. *Proc Natl Acad Sci U S A*. 2001;98:4605–4610.
16. Venkatesha S, Toporsian M, Lam C, Hanai J, Mammoto T, Kim YM, Bdolah Y, Lim KH, Yuan HT, Libermann TA, Stillman IE, Roberts D, D'Amore PA, Epstein FH, Sellke FW, Romero R, Sukhatme VP, Letarte M, Karumanchi SA. Soluble endoglin contributes to the pathogenesis of preeclampsia. *Nat Med*. 2006;12:642–649.
17. Lu F, Bytautiene E, Tamayo E, Gamble P, Anderson GD, Hankins GD, Longo M, Saade GR. Gender-specific effect of overexpression of sFlt-1 in pregnant mice on fetal programming of blood pressure in the offspring later in life. *Am J Obstet Gynecol*. 2007;197:418.e1–e5.
18. Lu F, Longo M, Tamayo E, Maner W, Al-Hendy A, Anderson GD, Hankins GD, Saade GR. The effect of over-expression of sFlt-1 on blood pressure and the occurrence of other manifestations of preeclampsia in unrestrained conscious pregnant mice. *Am J Obstet Gynecol*. 2007;196: 396.e1–e7.
19. Li Z, Zhang Y, Ying Ma J, Kapoun AM, Shao Q, Kerr I, Lam A, O'Young G, Sannajust F, Stathis P, Schreiner G, Karumanchi SA, Protter AA, Pollitt NS. Recombinant vascular endothelial growth factor 121 attenuates hypertension and improves kidney damage in a rat model of preeclampsia. *Hypertension*. 2007;50:686–692.
20. Espinoza J, Romero R, Nien JK, Gomez R, Kusanovic JP, Gonçalves LF, Medina L, Edwin S, Hassan S, Carstens M, Gonzalez R. Identification of patients at risk for early onset and/or severe preeclampsia with the use of uterine artery Doppler velocimetry and placental growth factor. *Am J Obstet Gynecol*. 2007;196:326.e1–326.e13.
21. Ohkuchi A, Hirashiama C, Matsubara S, Suziki H, Takahashi K, Arai F, Watanabe T, Kario K, Suzuki M. Alterations in placental growth factor levels before and after the onset of preeclampsia are more pronounced in women with early onset severe preeclampsia. *Hypertens Res*. 2007;30:151–159.
22. Krauss T, Pauer HU, Augustin HG. Prospective analysis of placenta growth factor (PlGF) concentrations in the plasma of women with normal pregnancy and pregnancies complicated by preeclampsia. *Hypertens Pregnancy*. 2004;23:101–111.
23. Kondo K, Hiratsuka S, Subbalakshmi E, Matsushime H, Shibuya M. Genomic organization of the flt-1 gene encoding for vascular endothelial growth factor (VEGF) receptor-1 suggests an intimate evolutionary relationship between the 7-Ig and the 5-Ig tyrosine kinase receptor. *Gene*. 1998;208:297–305.
24. Watanabe K, Hasegawa Y, Yamashita H, Shimizu K, Ding Y, Abe M, Ohta H, Imagawa K, Hojo K, Maki H, Sonoda H, Sato Y. Vasohibin as an endothelium-derived negative feedback regulator of angiogenesis. *J Clin Invest*. 2004;114:898–907.
25. Kamba T, Tam BY, Hashizume H, Haskell A, Sennino B, Mancuso MR, Norberg SM, O'Brien SM, Davis RB, Gowen LC, Anderson KD, Thurston G, Joho S, Springer ML, Kuo CJ, McDonald DM. VEGF-dependent plasticity of fenestrated capillaries in the normal adult microvasculature. *Am J Physiol Heart Circ Physiol*. 2006;290:H560–H576.
26. Yang JC, Haworth L, Sherry RM, Hwu P, Schwartzentruber DJ, Topalian SL, Steinberg SM, Chen HX, Rosenberg SA. A randomized trial of bevacizumab, an anti-vascular endothelial growth factor antibody, for metastatic renal cancer. *N Engl J Med*. 2003;349:427–434.
27. Hurwitz H, Fehrenbacher L, Novotny W, Cartwright T, Hainsworth J, Heim W, Berlin J, Baron A, Griffing S, Holmgren E, Ferrara N, Fyfe G, Rogers B, Ross R, Kabbinavar F. Bevacizumab plus irinotecan, fluorouracil, and leucovorin for metastatic colorectal cancer. *N Eng J Med*. 2004;350:2335–2342.
28. Escudier B, Eisen T, Stadler WM, Szczylik C, Oudard S, Siebels M, Negrier S, Chebreau C, Solska E, Desai AA, Rolland F, Demkow T, Hutson TE, Gore M, Freeman S, Schwartz B, Shan M, Simantov R, Bukowski RM; for the TARGET Study Group. Sorafenib in advanced clear-cell renal-cell carcinoma. *N Eng J Med*. 2007;356:125–134.
29. Chu TF, Rupnick MA, Kerkela R, Dallabrida SM, Zurakowski D, Nguyen L, Woulfe K, Pravda E, Cassiola F, Desai J, George S, Morgan JA, Harris DM, Ismail NS, Chen JH, Schoen FJ, Van den Abbeele AD, Demetri GD, Force T, Chen MH. Cardiotoxicity associated with tyrosine kinase inhibitor sunitinib. *Lancet*. 2007;370:2011–2019.
30. Li B, Ogasawara AK, Yang R, Wei W, He GW, Zioncheck TF, Bunting S, de Vos AM, Jin H. KDR (VEGF receptor 2) is the major mediator for the hypotensive effect of VEGF. *Hypertension*. 2002;39:1095–1100.
31. Yang R, Ogasawara AK, Zioncheck TF, Ren Z, He GW, DeGuzman GG, Pelletier N, Shen BQ, Bunting S, Jim H. Exaggerated hypotensive effect of vascular endothelial growth factor in spontaneously hypertensive rats. *Hypertension*. 2002;39:815–820.
32. Parsons-Wingerter P, Chandrasekharan UM, McKay TL, Radhakrishnan K, DiCorleto PE, Albarran B, Farr AG. A VEGF165-induced phenotypic switch from increased vessel density to increased vessel diameter and increased endothelial NOS activity. *Microvasc Res*. 2006;72:91–100.
33. Sandrim VC, Palei AC, Metzger IF, Gomes VA, Cavalli RC, Tanus-Santos JE. Nitric oxide formation is inversely related to serum levels of antiangiogenic factors soluble fms-like tyrosine kinase-1 and soluble endogline in preeclampsia. *Hypertension*. 2008;52:402–407.
34. Sibai BM, Mercer BM, Schiff E, Friedman SA. Aggressive versus expectant management of severe preeclampsia at 28 to 32 weeks' gestation: a randomized controlled trial. *Am J Obstet Gynecol*. 1994;171: 818–822.
35. Park JE, Chen HH, Winer J, Houck KA, Ferrara N. Placenta growth factor: potentiation of vascular endothelial growth factor bioactivity, in vitro and in vivo, and high affinity binding to Flt-1 but not to Flk-1/KDR. *J Biol Chem*. 1994;269:25646–25654.
36. Sawano A, Takahashi T, Yamaguchi S, Aonuma M, Shibuya M. Flt-1 but not KDR/Flk-1 tyrosine kinase is a receptor for placenta growth factor, which is related to vascular endothelial growth factor. *Cell Growth Differ*. 1996;7:213–221.
37. Osol G, Celia G, Gokina N, Barron C, Chien E, Mandala M, Luksha L, Kublickiene K. Placental growth factor is a potent vasodilator of rat and human resistance arteries. *Am J Physiol Heart Circ Physiol*. 2008;294: H1381–H1387.
38. Abid MR, Schoots IG, Spokes KC, Wu SQ, Mawhinney C, Aird WC. Vascular endothelial growth factor-mediated induction of manganese superoxide dismutase occurs through redox-dependent regulation of forkhead and IkappaB/NF-kappaB. *J Biol Chem*. 2004;279:44030–44038.
39. González-Pacheco FR, Deudero JJ, Castellanos MC, Castilla MA, Alvarez-Arroyo MV, Yagüe S, Caramelo C. Mechanisms of endothelial response to oxidative aggression: protective role of autologous VEGF and induction of VEGFR2 by H2O2. *Am J Physiol Heart Circ Physiol*. 2006;291:H1395–H1401.

Suppression of *Sproutys* Has a Therapeutic Effect for a Mouse Model of Ischemia by Enhancing Angiogenesis

Koji Taniguchi[1,2,3], Ken-ichiro Sasaki[4], Kousuke Watari[5], Hideo Yasukawa[4], Tsutomu Imaizumi[4], Toranoshin Ayada[1], Fuyuki Okamoto[1], Takuma Ishizaki[3], Reiko Kato[1], Ri-ichiro Kohno[6], Hiroshi Kimura[7], Yasufumi Sato[7], Mayumi Ono[5], Yoshikazu Yonemitsu[6,8], Akihiko Yoshimura[3,9]*

1 Division of Molecular and Cellular Immunology, Medical Institute of Bioregulation, Kyushu University, Fukuoka, Japan, **2** Department of Surgery and Science, Graduate School of Medical Sciences, Kyushu University, Fukuoka, Japan, **3** Department of Microbiology and Immunology, Keio University School of Medicine, Shinjuku-ku, Tokyo, Japan, **4** Division of Cardiovascular Medicine, Department of Internal Medicine, Kurume University, Kurume, Japan, **5** Department of Pharmaceutical Oncology, Graduate School of Pharmaceutical Sciences, Kyushu University, Fukuoka, Japan, **6** Division of Pathophysiological and Experimental Pathology, Department of Pathology, Graduate School of Medical Sciences, Kyushu University, Fukuoka, Japan, **7** Department of Vascular Biology, Institute of Development, Aging, and Cancer, Tohoku University, Sendai, Japan, **8** Department of Gene Therapy, Chiba University Graduate School of Medicine, Chiba, Japan, **9** Japan Science and Technology Corporation (JST), CREST, Kawaguchi, Japan

Abstract

Sprouty proteins (Sproutys) inhibit receptor tyrosine kinase signaling and control various aspects of branching morphogenesis. In this study, we examined the physiological function of Sproutys in angiogenesis, using gene targeting and short-hairpin RNA (shRNA) knockdown strategies. *Sprouty2* and *Sprouty4* double knockout (KO) (DKO) mice were embryonic-lethal around E12.5 due to cardiovascular defects. The number of peripheral blood vessels, but not that of lymphatic vessels, was increased in *Sprouty4* KO mice compared with wild-type (WT) mice. *Sprouty4* KO mice were more resistant to hind limb ischemia and soft tissue ischemia than WT mice were, because *Sprouty4* deficiency causes accelerated neovascularization. Moreover, suppression of *Sprouty2* and *Sprouty4* expression *in vivo* by shRNA targeting accelerated angiogenesis and has a therapeutic effect in a mouse model of hind limb ischemia. These data suggest that Sproutys are physiologically important negative regulators of angiogenesis *in vivo* and novel therapeutic targets for treating peripheral ischemic diseases.

Citation: Taniguchi K, Sasaki K-i, Watari K, Yasukawa H, Imaizumi T, et al. (2009) Suppression of *Sproutys* Has a Therapeutic Effect for a Mouse Model of Ischemia by Enhancing Angiogenesis. PLoS ONE 4(5): e5467. doi:10.1371/journal.pone.0005467

Editor: Rory Edward Morty, University of Giessen Lung Center, Germany

Received March 5, 2009; **Accepted** April 13, 2009; **Published** May 8, 2009

Funding: This study was supported by Grants-in-Aid for Scientific Research (S) and for Scientific Research on Priority Areas from the Ministry of Education, Culture, Sports, Science and Technology of Japan, the Program for Promotion of Fundamental Studies in Health Sciences of the National Institute of Biomedical Innovation (NIBIO), the Naito Foundation, and the Astellas Foundation for Research on Metabolic Disorders. The funders had no role in study design, data collection and analysis, decision to publish, or preparation of the manuscript.

Competing Interests: The authors have declared that no competing interests exist.

* E-mail: yoshimura@a6.keio.jp

Introduction

Growth factor-induced signaling by receptor tyrosine kinases (RTKs) plays several essential roles in development and pathogenesis; accordingly, it is tightly controlled by a number of regulatory proteins [1–3]. When a ligand binds to an RTK and recruits a Grb2-Sos to the inner surface of a membrane, the Sos protein binds to Ras, causing GDP/GTP exchange and thus activating Ras. Activated Ras recruits Raf to the plasma membrane and activates the Raf/MEK/extracellular signal-regulated kinase (ERK) pathway. Some growth factors, such as vascular endothelial growth factor (VEGF)-A, also activate the Raf/MEK/ERK pathway through the RTK/phospholipase C (PLC)-γ/protein kinase C (PKC) pathway, which is a Ras-independent pathway [4].

Sprouty (Spry) has been genetically identified as an antagonist of fibroblast growth factor (FGF) receptor in tracheal development in *Drosophila*, and is a proven negative regulator of the Ras/Raf/ERK pathway [5,6]. Four mammalian genes with sequence similarity to *Drosophila Sprouty* (*Sprouty1–4*) have been identified [1,2]. In addition, we have identified three Sprouty-related proteins known as Spred1–3 (Spreds), in which the C-terminal cysteine-rich domain found in Sprouty proteins (Sproutys) is conserved [7,8]. Since loss-of-function mutations of the *SPRED1* gene have been found in human neuro-cardio-facial-cutaneous (NCFC) syndromes [9], and since these syndromes are caused by dysregulation of the Ras-ERK pathway, we conclude that SPRED1 is a negative regulator of RTK-mediated Ras/ERK activation.

In the development of the cardiovascular system of *Drosophila*, as in the tracheal system, the formation of new blood vessels from preexisting ones (angiogenesis) involves the sprouting of endothelial cells out of an epithelial layer and the branching of tubular structures [10]. In the adult, angiogenesis only takes place during the female reproductive cycle, during wound healing, and in pathological situations, including tumor growth, diabetic retinopathy, arthritis, atherosclerosis, and psoriasis [10,11]. Angiogenesis is tightly regulated by a balance between inducing and inhibitory signals [12]. Growth factors, such as VEGF-A, basic FGF (bFGF), and angiopoietins, positively regulate angiogenesis by binding to

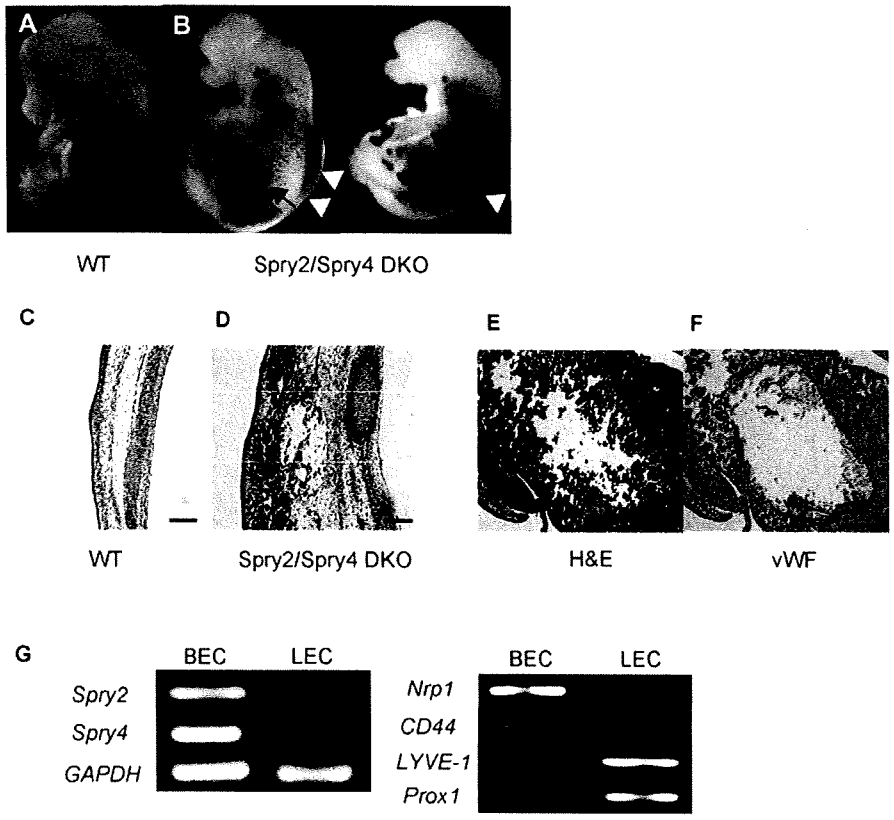

Figure 1. Characterization of *Sprouty2/Sprouty4* DKO mice. (A, B) Gross appearance of wild-type (WT) (A) and *Sprouty2/Sprouty4* DKO (B) embryos at embryonic day 12.5. The arrow and arrowheads indicate hemorrhage and edema, respectively. (C, D) Hematoxylin-eosin (H&E) staining of sections of WT (C) and *Sprouty2/Sprouty4* DKO (D) skin. (E, F) H&E staining and immunohistochemical staining with von Willebrand factor (vWF) of sections of hepatic hemangiomas in *Sprouty2/Sprouty4* DKO liver. vWF was used as a blood vessel marker. (G) Expression of *Sproutys* in endothelial cells. About 5.0×10^4 BECs and LECs were FACS-sorted at embryonic day 14.5, and were used for RT-PCR analysis. *GAPDH* served as a loading control. Good separation of BECs and LECs was confirmed by BEC markers (*Nrp1*, *CD44*) and LEC markers (*LYVE1*, *Prox1*). Scale bars (C–F): 100 μm.
doi:10.1371/journal.pone.0005467.g001

their cognate RTKs and thus inducing endothelial cell proliferation, migration, differentiation, and survival [12,13]. In addition, sphingosine-1-phosphate (S1P), which activates GPCRs, has also been implicated in angiogenesis [14]. In contrast, proteins that negatively regulate angiogenesis by specifically blocking RTK signaling are less well characterized.

Previous studies have demonstrated that overexpression of Sproutys inhibits VEGF-A- and bFGF-induced endothelial cell proliferation and differentiation *in vitro* as well as branching and sprouting of small vessels *in vivo* [15,16]. Moreover, Sprouty4 suppresses VEGF-A/VEGF receptor (VEGFR)-2 signaling *in vitro* [17–19]. We also know that Spreds, in contrast, inhibit VEGF-C signaling, which is important in lymphangiogenesis, and that *Spred1/Spred2* double knockout (KO) (DKO) mice show abnormal lymphatic development [18]. Yet the physiological role of Sproutys in angiogenesis and lymphangiogenesis remains to be elucidated.

In this study we investigated the physiological function of Sproutys in angiogenesis by performing knockout and knockdown analyses of *Sproutys*. We showed that Sproutys are negative regulators for angiogenesis rather than lymphangiogenesis *in vivo*. Moreover, *Sprouty4* KO mice were more resistant to hind limb ischemia and soft tissue ischemia than wild-type (WT) mice were, and *in vivo* shRNA targeting *Sprouty2* and *Sprouty4* accelerated angiogenesis in a mouse model of hind limb ischemia. These data suggest that Sprouty2 and Sprouty4 are important negative regulators of angiogenesis *in vivo* that could be new therapeutic targets for ischemic diseases.

Results

Increased developmental angiogenesis in *Sprouty*-deficient mice

Overexpression studies suggest that Sprouty2 and Sprouty4 possess similar negative effects on RTK-mediated ERK activation [20]. To define the overlapping functions of Sprouty2 and Sprouty4, we generated *Sprouty2/Sprouty4* DKO mice. *Sprouty2/Sprouty4* DKO mice were embryonic-lethal by embryonic day 12.5 and showed very severe defects in craniofacial and limb morphogenesis [21]. They also showed very severe subcutaneous hemorrhage, edema (Fig. 1A–D), and multiple hepatic hemangiomas (Fig. 1E,F), which suggested that they had cardiovascular defects as well. We next investigated the expression pattern of *Sprouty2* and *Sprouty4* in endothelial cells during embryonic development, and found that *Sprouty2* and *Sprouty4* were more highly expressed in blood endothelial cells (BECs) than in lymphatic endothelial cells (LECs) (Fig. 1G).

This discovery led us to examine vascularization in adult *Sprouty4* single KO mice in detail, although *Sprouty4* single KO

mice showed no obvious vascular phenotype [21]. *Sprouty4* single KO mice exhibited more vascular networks of blood vessels in the ear than WT mice did (Fig. 2A,B). Similarly, more vascular networks of blood vessels in the ear were observed in *Sprouty2* single KO mice than in WT mice (data not shown). The numbers of blood vessels in the skin were also increased in *Sprouty4* KO mice (Fig. 2C,D). Lymphatic vessel networks, on the other hand, were present at the same frequency in these *Sprouty4* KO mice as in WT mice (Fig. 2A–D). Retinal vasculature is a good model system for the study of general blood vessel development [22]. Vascular development in the early embryo is difficult to observe, but the murine retinal vascular system develops after birth and is therefore easier to examine. We compared flat-mounted retinas from WT and *Sprouty4* KO mice at postnatal day (PD) 3 after injecting FITC-dextran (Fig. 2E). As the image clearly shows, retinal angiogenesis was enhanced in *Sprouty4* KO mice compared to WT mice.

These data suggest that, in contrast to Spred1 and Spred2, which are important negative regulators of developmental lymphangiogenesis rather than developmental angiogenesis, as previously reported [18], Sprouty2 and Sprouty4 are important negative regulators of developmental angiogenesis rather than developmental lymphangiogenesis.

Sprouty4 KO mice are more resistant to ischemia

Next, we sought to investigate the effect of *Sprouty4* deficiency in the ischemia-induced angiogenesis model, an adult neovascularization assay which is useful for quantifying neovascularization in *Sprouty4* KO mice. We used mouse models of hind limb ischemia [23] and soft tissue ischemia [24]. We used *Sprouty4* KO mice, since *Sprouty4* KO mice can survive much longer than *Sprouty2* KO mice [21,25].

The former model revealed that *Sprouty4* KO mice were more resistant to hind limb ischemia than WT mice were (Fig. 3A). *Sprouty4* KO mice showed a significantly elevated recovery of limb perfusion after induction of hind limb ischemia as compared with WT mice, and the ischemic/non-ischemic leg perfusion ratio was much more favorable in *Sprouty4* KO mice than in WT mice ($P<0.001$) (Fig. 3B,C). Additionally, angiogenesis in the ischemic hind limb was significantly increased in *Sprouty4* KO mice compared with WT mice (Fig. 3D).

The latter model was induced by creating lateral skin incisions on the dorsal surfaces of mice. The overlying skin was undermined, and a silicone sheet was inserted into each mouse to separate the skin from the underlying tissue bed. As a result, the most central portion of skin underwent the most severe ischemic insult, which, in WT mice, ultimately led to the absence of flow and necrosis in the central portion of the skin (Fig. 4A). In *Sprouty4* KO mice, however, angiogenesis in the dorsal skin was significantly increased compared to that in WT mice (Fig. 4B). As a result, *Sprouty4* KO mice were more resistant to soft tissue ischemia than WT mice were, and gross evidence of necrosis in the dorsal skin was more evident in WT mice than in *Sprouty4* KO mice (100% and 16.7% in WT mice and *Sprouty4* KO mice, respectively, n = 6) (Fig. 4A).

These data show that *Sprouty4* KO mice exhibit enhanced neovascularization in ischemia-induced models.

Increased ischemia-induced neovascularization by *in vivo* shRNA targeting *Sproutys*

The increased vessel density in the skin and muscles of untreated *Sprouty4* KO mice (Fig. 2C,D, Fig. 3D) provides them with elevated blood-vessel area in these regions, which is partially responsible for their increased resistance to ischemia.

To investigate *in vivo* the efficiency of down-regulating *Sproutys* as therapy for peripheral ischemic diseases, we administered ischemia treatment to the hind limbs of C57BL/6J mice, then injected shRNA targeting *Sprouty2* and *Sprouty4*. We suppressed both *Sprouty2* and *Sprouty4* simultaneously, because both of the mRNAs increased during hind limb ischemia (Fig. 5A), because the phenotype of *Sprouty2*/*Sprouty4* DKO mice demonstrated a redundant role of *Sprouty2* and *Sprouty4* in angiogenesis (Fig. 1), and because we have not found any functional differences between Sprouty2 and Sprouty4 *in vitro* [20]. The shRNA plasmid targeting *Sprouty2* and *Sprouty4* efficiently suppressed the expression levels of endogenous Sprouty2 and Sprouty4, respectively, in both real-time PCR (Fig. 5B,C) and Western blot (Fig. 5D,E) analysis. The shRNA plasmids targeting both *Sprouty2* and *Sprouty4* enhanced VEGF-A-induced ERK and Akt activation *in vitro* in mouse embryonic fibroblasts (MEFs), which stably expressed VEGFR-2 (Fig. 5F). We used MEFs because it has been very difficult to introduce shRNA into primary murine endothelial cells *in vitro*. Although we confirmed that shRNA against Sprouty2 or Sprouty4 alone enhanced VEGF-A-induced ERK and Akt activation (data not shown), we observed much stronger effect by the combination of Sprouty2 and Sprouty4 shRNAs. Thus we decide to use combination of both Sprouty2 and Sprouty4 shRNAs for further experiments.

First, we showed that injection of shRNA plasmids targeting *Sprouty2* and *Sprouty4* significantly enhanced corneal neovascularization induced by VEGF-A, compared to control shRNA plasmids in a corneal micropocket assay (Fig. 6A–C). These data indicate that *Sprouty2* and *Sprouty4* shRNA plasmids can efficiently suppress the expression levels of Sprouty2 and Sprouty4 and block the effect of endogenous Sprouty2 and Sprouty4 *in vitro* and *in vivo*.

Next, we investigated whether *Sprouty2* and *Sprouty4* shRNA plasmids were effective in a mouse model of hind limb ischemia. Upon injection to the ischemic adductor muscle, *Sprouty2* and *Sprouty4* shRNA plasmids reduced *Sprouty2* and *Sprouty4* expression *in vivo* (Fig. 5A). *Sprouty2* and *Sprouty4* shRNA plasmids induced a significantly elevated recovery of limb perfusion after induction of hind limb ischemia as compared with control shRNA plasmids, and markedly improved the ischemic/non-ischemic leg perfusion ratio ($P<0.05$) (Fig. 7A,B). shRNA plasmids targeting *Sprouty2* and *Sprouty4* also increased capillary density compared with control shRNA plasmids (Fig. 7C). Our data clearly demonstrate that Sprouty2 and Sprouty4 negatively regulate angiogenesis *in vivo* and would make good therapeutic targets for peripheral ischemic diseases.

Discussion

In this study, we investigated the physiological function of Sproutys in angiogenesis by performing a knockout and knockdown analysis of *Sproutys*. In contrast to Spred1 and Spred2, which regulate developmental lymphangiogenesis, Sprouty2 and Sprouty4 are important negative regulators of developmental angiogenesis *in vivo*. We found that the amounts of blood vessels in *Sprouty4* KO mice are increased in all tissues we investigated. So we think that all peripheral blood vessels are increased in *Sprouty4* KO mice. *Sprouty4* deficiency enhanced ischemia-induced angiogenesis in mouse models of hind limb ischemia and soft tissue ischemia. Moreover, the suppression of *Sprouty2* and *Sprouty4* expression *in vivo* by shRNA targeting had a therapeutic effect in our model of hind limb ischemia, indicating that Sproutys should be novel therapeutic targets for treating peripheral ischemic diseases.

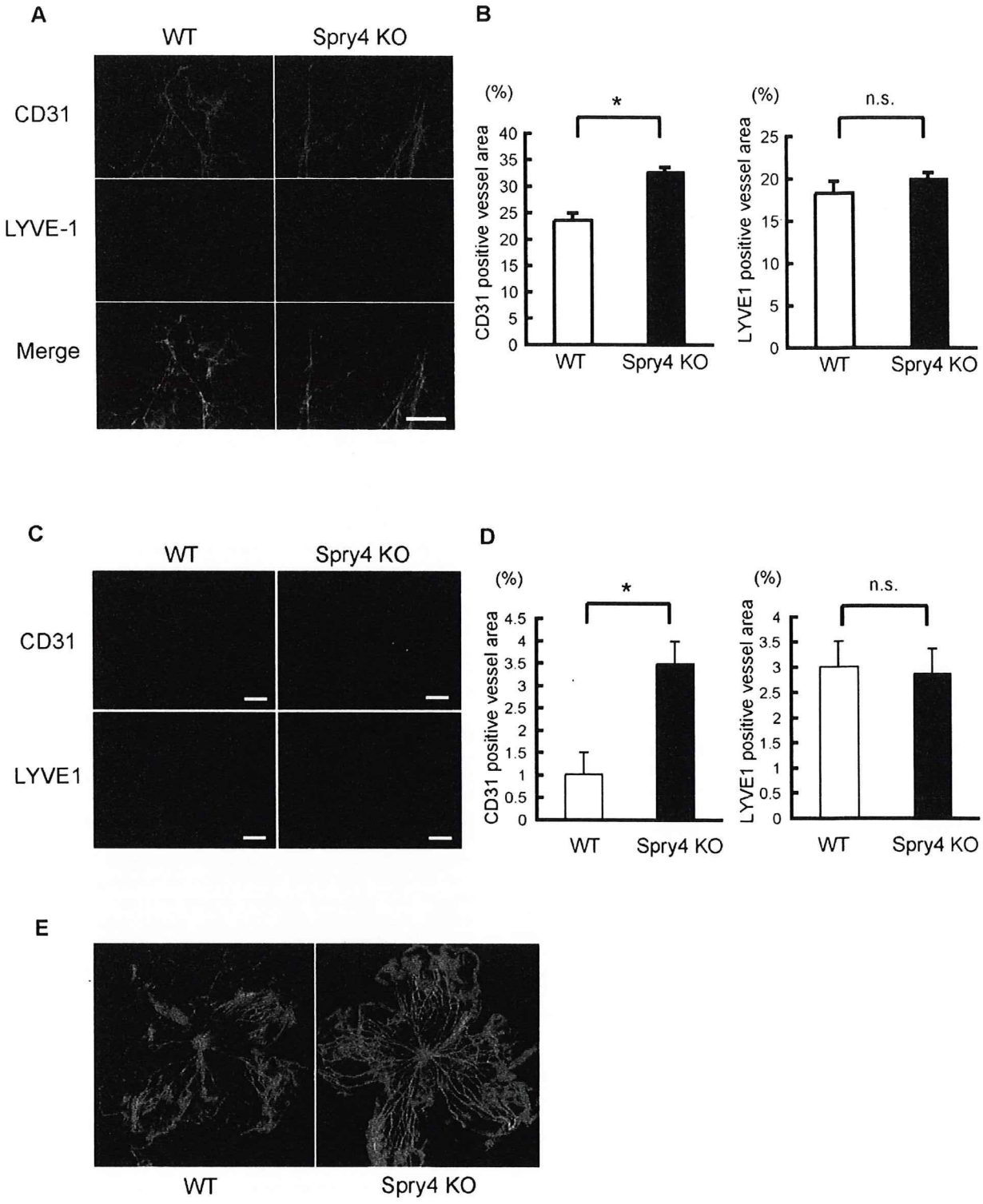

Figure 2. Blood and lymphatic vessels of *Sprouty4* single KO mice. (A) Blood vessels (green) and lymphatic vessels (red) in the ears of WT and *Sprouty4* KO mice (8 weeks old) were analyzed by whole-mount immunohistochemical staining with anti-PECAM-1/CD31Ab and anti-LYVE-1 Ab, respectively. (B) CD31-positive vessel area or LYVE1-positive area was quantified. Data shown are means±SEM. *: $P<0.05$. (C) Blood vessels (green) and lymphatic vessels (red) in the dorsal skin of WT and *Sprouty4* KO mice (8 weeks old) were analyzed by immunohistochemical staining with anti-PECAM-1/CD31Ab and anti-LYVE-1 Ab, respectively. Nuclei were stained with Hoechst 33342 dye (Blue). (D) CD31-positive vessel area or LYVE1-positive area was quantified. Data shown are means±SEM. *: $P<0.05$. (E) FITC-dextran-perfused flat-mounted retinal samples of WT and *Sprouty4* KO mice at postnatal day 3. Scale bars (A, C): 100 μm.
doi:10.1371/journal.pone.0005467.g002

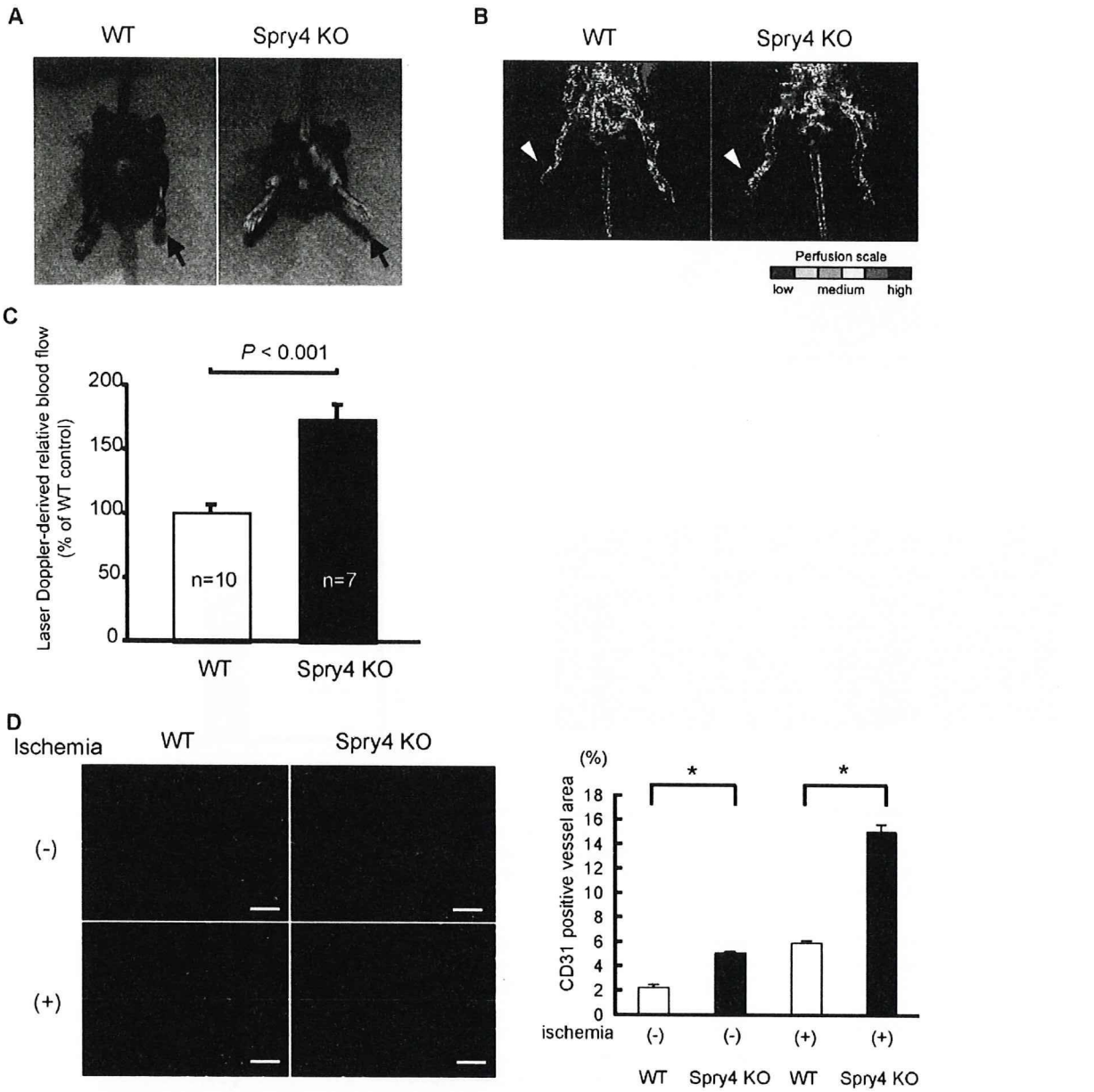

Figure 3. *Sprouty4* KO mice are more resistant in a hind-limb ischemia model. (A) Representative photos of ischemic limbs, indicated by arrows. (B) Representative laser Doppler images for each group are depicted. Arrowheads indicate ischemic limbs. The interval of low perfusion is displayed as dark blue; the highest perfusion interval is displayed as red. (C) Recovery of limb perfusion in WT (n = 10) and *Sprouty4* KO (n = 7) mice after hind limb ischemia as assessed by laser Doppler blood flow analysis on day 14. Data shown are means±SD. *: $P<0.001$. (D) Blood vessels (green) in the non-ischemic or ischemic adductor muscles of male WT and *Sprouty4* KO mice (8–10 weeks old) were analyzed by immunohistochemical staining with anti-PECAM-1/CD31Ab. Nuclei were stained with Hoechst 33342 dye (blue). The CD31-positive vessel area was quantified. Data shown are means±SEM. *: $P<0.05$. Scale bars: (D) 100 μm.
doi:10.1371/journal.pone.0005467.g003

The roles of Sprouty and Spred proteins during gastrulation in *Xenopus tropicalis* have been compared elsewhere [26]. Spred proteins preferentially inhibit the Ras/ERK cascade that directs mesoderm formation, whereas Sprouty proteins block the Ca^{2+} and PKCδ signals required for morphogenetic movements during gastrulation. Thus, the expression of *Sprouty* and *Spred* genes at specific times during gastrulation might redirect FGF signals toward mesoderm formation or morphogenesis, respectively [26].

In mammalian development, *Sproutys* are expressed mainly in blood endothelial cells, while *Spreds* are expressed mainly in lymphatic endothelial cells (Fig. 1G and Ref. [18]). In overexpression experiments, while Sproutys can inhibit VEGF-A signaling but not VEGF-C signaling, Spreds can suppress both types (Taniguchi K., unpublished data and Ref. [18]). Indeed, microRNA-126 deletion suppresses VEGF-A-induced ERK activation in endothelial cells and angiogenesis through the increase of

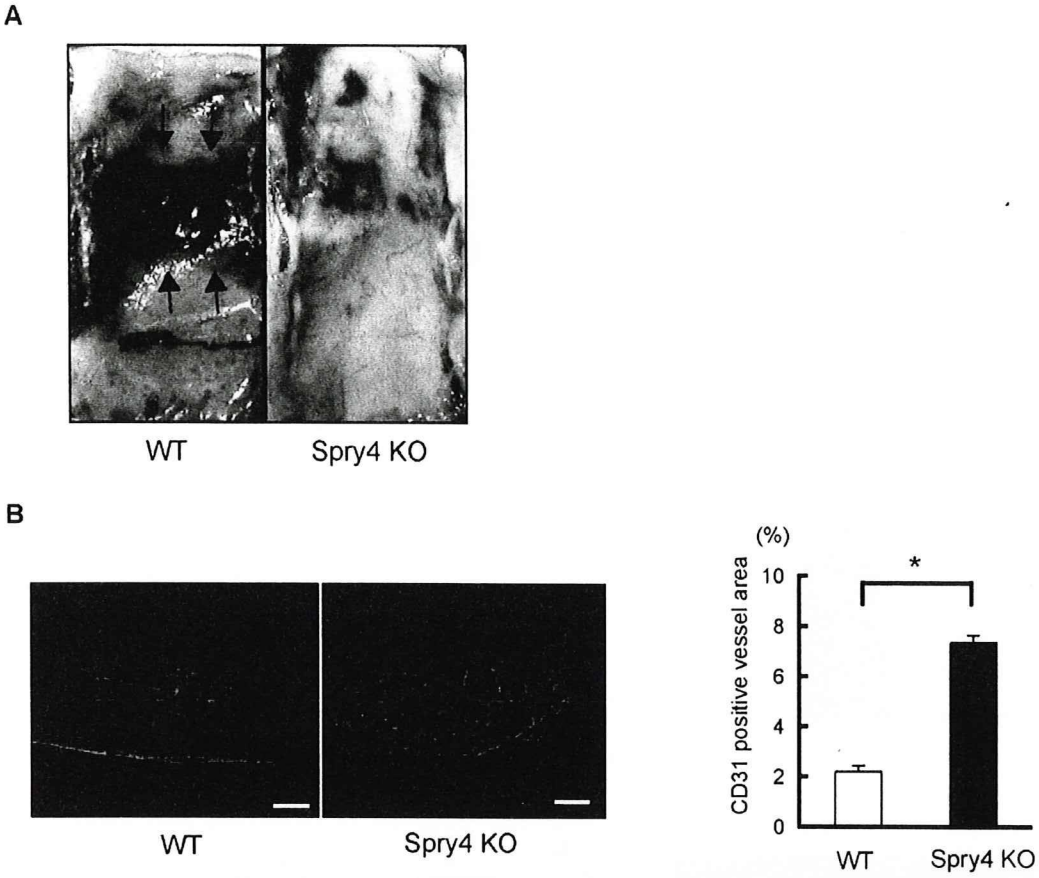

Figure 4. *Sprouty4* KO mice are also more resistant in a soft tissue ischemia model. (A) Representative photos of ischemic dorsal skin of male WT and *Sprouty4* KO mice (8–10 weeks old). Arrows indicate necrotic skin. (B) Left: Blood vessels (green) in the ischemic dorsal skin of male WT and *Sprouty4* KO mice were analyzed by immunohistochemical staining with anti-PECAM-1/CD31Ab. Nuclei were stained with Hoechst 33342 dye (blue). Right: The CD31-positive vessel area was quantified. Data shown are means±SEM. *: $P<0.05$. Scale bars (B): 100 μm.
doi:10.1371/journal.pone.0005467.g004

Spred1 [27–29]. However, the effect of *Sprouty* deletion is more specific to VEGF-A signaling than to VEGF-C signaling, while the effect of *Spred* deletion is more specific to VEGF-C signaling than to VEGF-A signaling (Taniguchi K., unpublished data and Ref. [18]). In fact, *Sprouty2* and *Sprouty4* single-deficient mice showed defects of blood vessels rather than lymphatic vessels, while *Spred1/Spred2* DKO mice showed abnormal lymphatic vessel development and nearly normal blood vessel development (Fig. 2 and Ref. [18]). In addition to this difference in expression, these results suggest that Sproutys and Spreds might have different functions in endothelial cells. VEGF-A/VEGFR-2 signaling is Ras-independent and PLC-γ/PKC-dependent, while VEGF-C/VEGFR-3 signaling is Ras-dependent and PKC-independent (Taniguchi K., unpublished data and Ref. [4]). Therefore, drawing an analogy from the different functions of Sproutys and Spreds in *Xenopus tropicalis*, we propose that Sproutys inhibit PLC-γ/PKC-dependent VEGF-A signaling and angiogenesis, while Spreds inhibit Ras-dependent VEGF-C signaling and lymphangiogenesis.

Although, in ischemia-induced angiogenesis, VEGF-A is thought to be the primary angiogenesis-stimulating factor [30], angiogenesis is the more complex process, as it is triggered not only by VEGF-A but also by bFGF, S1P, angiopoietins, and others [12–14]. In fact, it is reported that *bFGF* gene therapy is effective to treat critically ischemic limb [31]. It is already known that Sproutys can inhibit various RTK signals [1,2]. We have also shown that loss of *Sprouty* expression results in hyperactivation of VEGF-A and bFGF signaling as well as S1P and LPA signaling (Fig. 5F, Taniguchi K., unpublished data and Ref. [19] and [21]). It is reported that *in vivo* shRNA targeting *SHP-1* also accelerated angiogenesis in a rat model of hind limb ischemia [32]. While SHP-1 inhibits only RTK signals, Sproutys suppress both RTK and GPCR signals. Thus the suppression of *Sproutys* could be beneficial.

Inhibition of negative feed-back loops leading to profound and long term activation of signals often lead to a dysregulation of neovascularisation since the overshooting response is inducing immature vessels. However, excessive sprouting in response to inhibition of Sproutys results in the formation of mature vessels. Angiogenesis is a complex process that includes the recruitment and proliferation of various cells, such as endothelial cells, mural cells [smooth muscle cells (SMC) and pericytes], endothelial progenitor cells (EPCs) and others. It is reported that *Sprouty*-family genes are expressed in both endothelial cells and smooth muscle cells [33], and we have confirmed that *Sprouty/Spred* family genes are also expressed in bone marrow (Taniguchi K., unpublished data). It is possible that Sproutys function not only in endothelial cells, but also in mural cells, EPCs or myeloid cells, and that enhanced angiogenesis of mature vessels in *Sprouty4* KO mice and

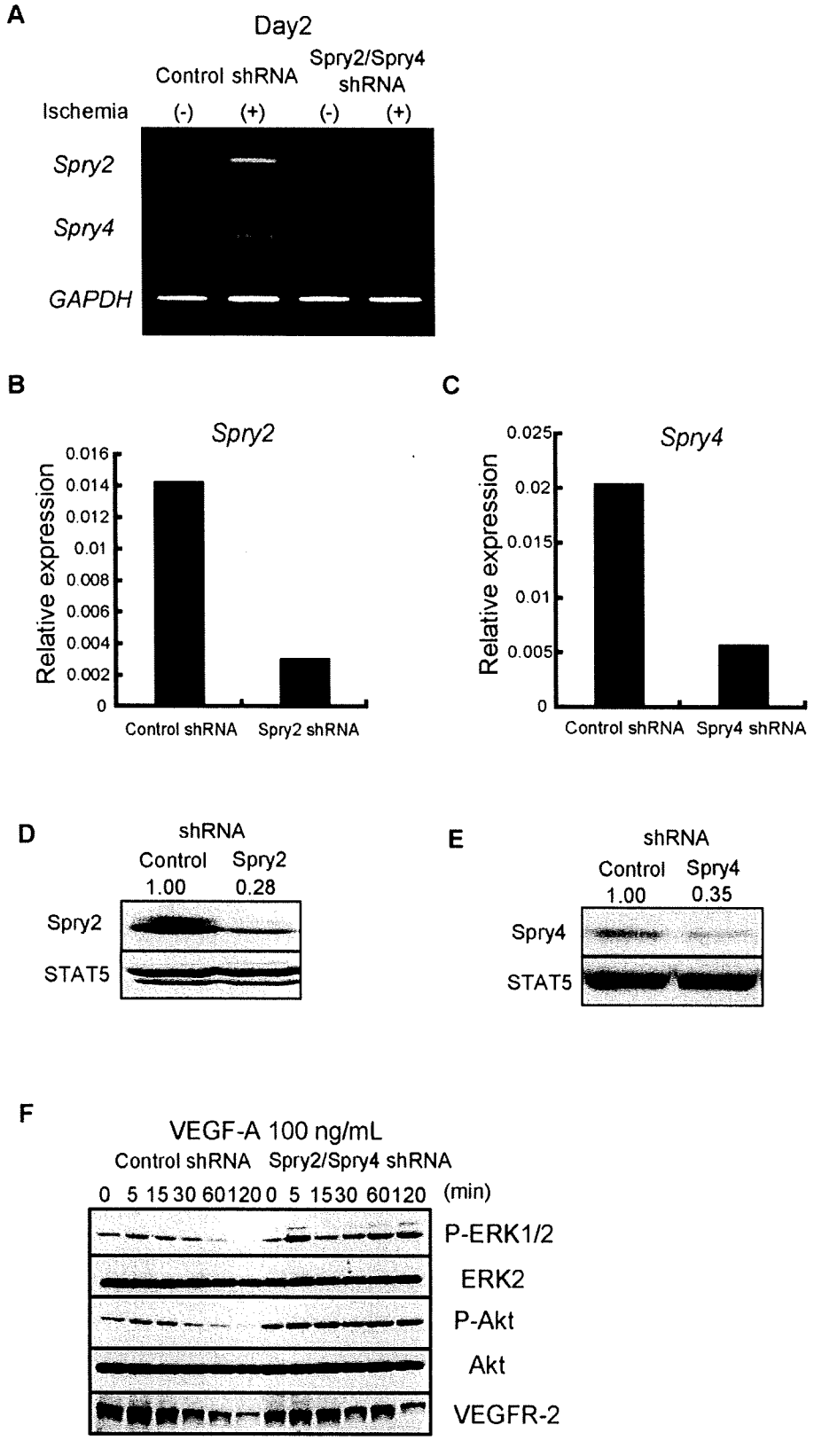
A
Day2
Control shRNA
Spry2/Spry4 shRNA
Ischemia
(-)
(+)
(-)
(+)
Spry2
Spry4
GAPDH
B
Spry2
Relative expression
0.016
0.014
0.012
0.01
0.008
0.006
0.004
0.002
0
Control shRNA
Spry2 shRNA
C
Spry4
Relative expression
0.025
0.02
0.015
0.01
0.005
0
Control shRNA
Spry4 shRNA
D
shRNA
Control
Spry2
1.00
0.28
Spry2
STAT5
E
shRNA
Control
Spry4
1.00
0.35
Spry4
STAT5
F
VEGF-A 100 ng/mL
Control shRNA
Spry2/Spry4 shRNA
0 5 15 30 60 120 0 5 15 30 60 120
(min)
P-ERK1/2
ERK2
P-Akt
Akt
VEGFR-2

Figure 5. ***In vivo*** **effects of shRNA targeting** ***Sprouty2*** **and** ***Sprouty4.*** (A) The *in vivo* effects of shRNA plasmids targeting *Sproutys* in the hind limb model were evaluated by RT-PCR analysis. (B, C) Real-time PCR analysis of *Sprouty2* (B) or *Sprouty4* (C) mRNA expression in MEFs stably infected with control retroviruses and retroviruses expressing either *Sprouty2* shRNA (B) or *Sprouty4* shRNA (C). (D, E) Western blot analysis of protein extracts from MEFs stably infected with control retroviruses and retroviruses expressing either *Sprouty2* shRNA (D) or *Sprouty4* shRNA (E). The relative intensities of Sprouty2 and Sprouty4 bands normalized by STAT5 expression levels are shown above. (F) Effect of both *Sprouty2* and *Sprouty4* knockdown on ERK and Akt activities. MEFs stably expressing VEGFR-2 were infected with control retroviruses and retroviruses expressing *Sprouty2/Sprouty4* shRNA, and stimulated with 100 ng/mL VEGF-A. Cell extracts were immunoblotted with the indicated antibodies.
doi:10.1371/journal.pone.0005467.g005

the results of our experiments with *in vivo* shRNA targeting *Sproutys* are partially dependent on the enhanced function or the increased number of mural cells, EPCs or myeloid cells. Moreover, it is possible that Sproutys are also associated with angiopoietins signals, which are important for the maturation of blood vessels. Further study is necessary to investigate these possibilities.

Sprouty4 KO mice were more resistant to ischemia than WT mice were in mouse models of ischemia (Fig. 3, Fig. 4), and neovascularization induced by a tumor transplantation model was also accelerated by *Sprouty4* deficiency (Taniguchi K., unpublished data). Moreover, *in vivo* shRNA targeting *Sprouty2* and *Sprouty4* accelerated angiogenesis in a mouse model of hind limb ischemia (Fig. 7). In this study, muscle tissue injected with the *Sproutys* shRNA vectors exhibited a significant decrease in *Sproutys* transcripts (Fig. 5A). This knockdown efficiency may be due to the fact, in skeletal muscle, the efficiency of intramuscular gene transfer has been shown to be augmented from five- to seven-fold when the injected muscle is ischemic [34]. The present study is the first to uncover these significant implications for gene therapy using the *Sprouty2* and *Sprouty4* shRNA vectors for the treatment of peripheral ischemic diseases. The fact that Sproutys exhibit such broad suppression activity, inhibiting a wide variety of angiogenic factors and cells, indicates that the suppression of *Sproutys* must enhance neovascularization.

In conclusion, Sproutys are physiologically important regulators of angiogenesis *in vivo* and may be useful as new therapeutic targets for peripheral ischemic diseases.

Methods

Mice

Sprouty2 KO mice and *Sprouty4* KO mice have been described previously [21,25]. *Sprouty2* KO mice and *Sprouty4* KO mice were generated as 129/C57BL/6J mixed background, and then backcrossed into C57BL/6J at least five times. Gender-matched, WT littermates were used as controls. All experiments using these mice were approved by and performed according to the guidelines of the Animal Ethics Committee of Kyushu University, Fukuoka, Japan.

Cell culture

Primary mouse embryonic fibroblasts (MEFs) were prepared, as previously described [21]. MEFs were cultured in Dulbecco's modified Eagle's medium (DMEM) (Gibco, Grand Island, NY, USA) supplemented with 10% fetal bovine serum, penicillin and streptomycin. To generate MEFs stably expressing VEGFR-2 or shRNAs, MEFs were infected with the retroviruses produced by

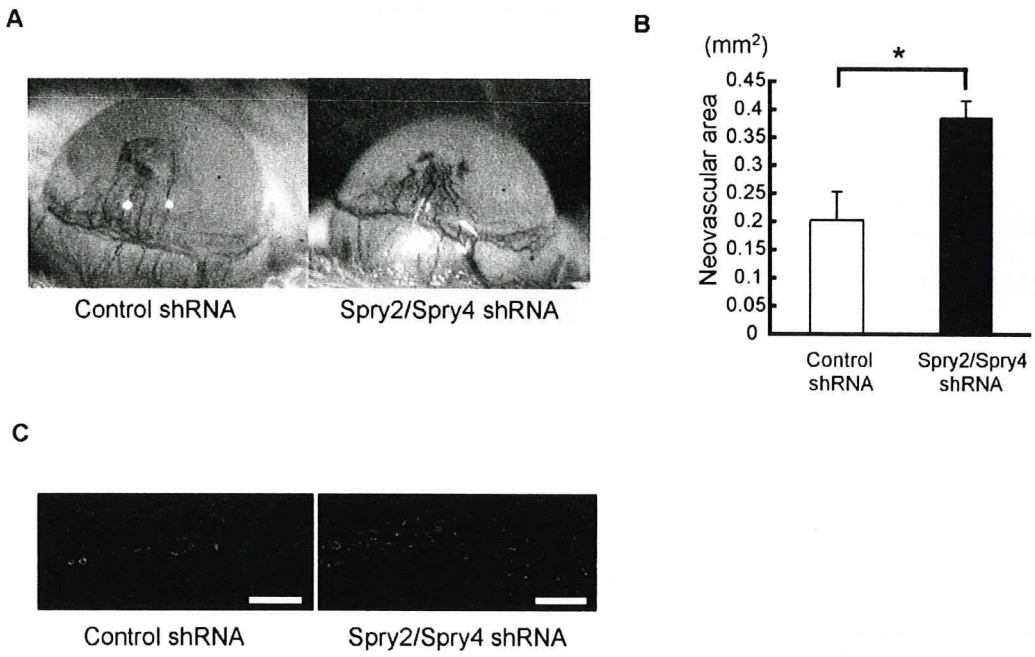

Figure 6. ***In vivo*** **effects of shRNA targeting** ***Sprouty2*** **and** ***Sprouty4*** **in corneal micropocket assay.** (A) Corneal neovascularization was induced by mouse VEGF-A (200 ng) on day 12 after hydron pellets had been implanted into male BALB/c mouse corneas. After implantation, 10 μg shRNA plasmids per eye were delivered by subconjunctival injection. Representative photos are shown. (B) Quantitative analysis of neovascularization on day 12. Areas are expressed in mm^2. Bars show the mean±SEM (n=5). *: $P<0.05$. (C) Sections of corneas implanted with VEGF-A stained by anti-PECAM-1/CD31Ab on day 12. Scale bars (C): 100 μm.
doi:10.1371/journal.pone.0005467.g006